

Evaluation of Photocatalysis for Gas-Phase Air Cleaning – Part 1: Process, Technical and Sizing Considerations

Dean T. Tompkins, PhD, PE (ASHRAE Member)

Ben J. Lawnicki, BS

Walter A. Zeltner, PhD

Marc A. Anderson, PhD

ABSTRACT

The results of a literature survey and an engineering analysis are presented that evaluate the process, technical and sizing considerations of photocatalytic oxidation (PCO) as a commercial technology to treat (i.e., remove) low-level contaminants in feed streams of air. PCO uses the energy of photons from light sources to activate a catalyst. Upon activation, adsorbed gases, particularly molecular oxygen (O₂), water vapor (H₂O), and contaminant species, can participate in surface-mediated reactions that, under appropriate operating conditions, can produce and desorb product species, notably carbon dioxide (CO₂) and H₂O. Approximately 60 organic compounds have been studied in heterogeneous gas-phase PCO, while only a few inorganic compounds have been studied. With regard to commercial-scale applications, the present challenge is to design photocatalytic treatment devices that have low pressure drop, make efficient use of light, and employ a stable catalyst that can be readily re-generated if it becomes poisoned or deactivated. Presently, gas-phase heterogeneous photocatalysis has a bright future for penetrating the most promising markets.

KEYWORDS: Air cleaning, air pollution control, catalysis, chemistry, contaminant, environmental control, filtration, gas, indoor air quality

D.T. Tompkins is associate scientist, Water Science and Engineering Laboratory, University of Wisconsin – Madison, Madison, WI; B.J. Lawnicki is process engineer, Intel Massachusetts, Hudson, MA; W.A. Zeltner is associate scientist, Water Science and Engineering Laboratory, University of Wisconsin – Madison, Madison, WI; M.A. Anderson is professor, Department of Civil and Environmental Engineering, University of Wisconsin – Madison, Madison, WI.

INTRODUCTION

Over the past quarter century, construction practices have favored the design of *tight* buildings and residences to reduce energy costs associated with the conditioning of building air. However, in the absence of sufficient ventilation, it is possible to increase the concentration of these volatile organic compounds (VOCs). This concern is exacerbated due to the significant percentage of time people spend in indoor environments. Indoor air contamination by undesired VOCs is a possible causative agent of the sick building syndrome. The 1989 OSHA workplace Time Weighted Average Permissible Exposure Limits (TWA-PEL) for exposure to VOCs during a 5-day-work week are in the range of 1 – 500 ppm in air (Plog 1988).

One approach to achieve air that contains lower concentrations of gas-phase contaminants is to employ UV catalytic technology or photocatalytic oxidation (PCO). PCO has gained attention in recent years as an approach to treat gaseous pollutants. The oxidant used in PCO is the 20% of oxygen present in air. Because the concentration of oxygen in air is so much larger than the (total) concentration of gaseous indoor air pollutants, it is not necessary to employ additional oxidants such as ozone (O₃) or hydrogen peroxide (H₂O₂).

In this paper, the results of a literature survey and an engineering analysis are presented that evaluate the process, technical and sizing considerations of PCO as a technology to treat contaminants in feed streams of air.

MAIN BODY

Photocatalytic Oxidation

Semiconductor materials provide solid surfaces that can influence both the chemical reactivity of a wide range of adsorbates and the ability to initiate, propagate, and terminate light-induced oxidation-reduction (redox) reactions – or PCO. Upon photoexcitation of several semiconductors, simultaneous redox reactions occur. The conversion often accomplishes either a specific, selective oxidation or a complete oxidative degradation of an organic reactant, in which the carbon bound in the reactant species

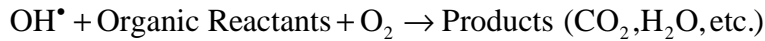
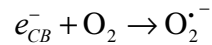
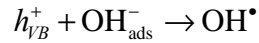
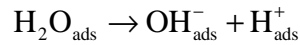
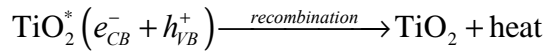
is converted to carbon dioxide. Molecular oxygen (O_2) is typically the oxidizing agent as has been demonstrated unmistakably in a few gas/solid reactions. Incident photons from light sources that initiate these reactions are in a wavelength region varying from the visible (~500 nm) to high-energy range of the UV spectrum (~250 nm), depending upon the band-gap of the photocatalyst. The semiconductor material that acts as the photocatalyst is often stable to the photolysis conditions, particularly when a metal oxide is employed. Though photocatalytic reactions can occur in both gas and liquid phases, the focus of this paper is on those reactions where gas-phase species are adsorbed and then react on solid surfaces, referred to as *heterogeneous* (gas/solid) photocatalysis (Serpone and Pelizzetti 1989).

Interest in photoinduced redox reactions originated with the observations of Fujishima and Honda (Fujishima and Honda 1972). They demonstrated that water could be split via a redox reaction upon illuminating a single-crystal semiconductor electrode made of titanium dioxide (TiO_2) to which a small electrochemical bias had been applied. These observations prompted extensive work focusing on the production of hydrogen from water as a means of solar energy conversion. It soon became apparent that novel redox reactions of organic and other inorganic substrates (Fox 1983, Fox 1991, Fox et al. 1991) could also be induced by band-gap irradiation of a variety of semiconductor materials varying in size from clusters and colloids to powders and large single crystals. Scientific interest in these chemical redox reactions has also developed within the last two decades because of the use of photoexcited semiconductor dispersions in chemistries that can find application in environmental protection (Alpert et al. 1991, Bahnemann et al. 1991, Blake et al. 1991, Matthews 1987, Ollis 1985, Schiavello 1988).

Basis of Photocatalysis

During the past quarter century, increasing research focus has been directed to the study of reactions on the illuminated semiconductor surface of metal oxides and sulfides consisting mainly of titanium dioxide (TiO_2), zinc oxide (ZnO), zirconium dioxide (ZrO_2), tungsten tri-oxide (WO_3), and cadmium sulfide (CdS). These materials have a moderate band-gap (1-3.3 eV) between their valence and conduction bands. When the semiconductor is illuminated by photons of energy $h\nu$ equal to or greater

than the band-gap E_g , the semiconductor absorbs the photons. This process excites the valence-band (VB) electrons to the conduction band (CB), creating highly reactive *electron* (e_{CB}^-) – *hole* (h_{VB}^+) charge carriers. When these charge carriers successfully migrate to the solid surface without recombining, the electrons and holes may undergo electron-transfer processes with adsorbates of suitable redox potentials (Fig. 1). Adsorbed water can react with holes to form highly reactive hydroxyl radicals (OH^\bullet), which in turn can oxidize organic compounds. Under certain reaction conditions, organic reactants can be completely oxidized (or mineralized) to form carbon dioxide, water, etc. as final products. The equations below describe a possible reaction pathway. The steps are represented as a series of reactions using TiO_2 as the semiconductor:



where ads = species adsorbed on semiconductor. A more detailed description of these processes along with characteristic times for charge-carrier generation (fs), charge-carrier trapping (100 ps to 10 ns), charge-carrier recombination (10 to 100 ns), and interfacial charge transfer (100 ns to ms) is reported in Hoffman et al. (1995). The quantum efficiency is determined by two critical processes – competition between charge-carrier recombination and trapping (picoseconds to nanoseconds) followed by the competition between recombination of trapped charge carriers and interfacial charge transfer of charge

carriers to reactants (since H_2O and O_2 are reactants) (microseconds to milliseconds) (Hoffman et al. 1995).

The first published report of photoreactivity was made by Renz (1921). However, heterogeneous photocatalysis studies only began in earnest in 1971 with the work of Teichner's group (Gravelle et al. 1971, Formenti et al. 1971) and Stone's group (Bickley et al. 1973). These studies provided the early vision for numerous potential applications of heterogeneous PCO. Studies involving gas-phase heterogeneous PCO are relatively few in number compared with the published studies of the photocatalytic treatment of compounds in aqueous media (Matthews 1982, Ollis et al. 1991, Serpone & Pelizzetti, 1989). However, there is increasing interest in gas-solid heterogeneous PCO because of the potential application to contaminant control in indoor environments including residences, office buildings, factories, aircraft, and spacecraft. The promise held by heterogeneous PCO lies in the moderate operating conditions required to initiate redox reactions. The semiconductors mentioned above have proved to be effective photocatalysts for performing surface-mediated reactions in which many organics are converted to CO_2 and H_2O (Peral et al. 1997). For example, the two predominant photocatalyst compounds in the literature, TiO_2 and ZnO , operate under the following favorable circumstances (Peral et al. 1997):

1. Photoactivation by near UV (wavelength (λ) range is ~300-370 nm) illumination, which allows for consideration of solar as well as artificial photon sources like fluorescent lights.
2. The catalyst materials are generally safe – TiO_2 is found in toothpastes and house paints, and is used as a sun-block agent.
3. The oxygen source is O_2 in air, which is present in enormous stoichiometric excess (210,000 ppm) compared with 1-500 ppm oxidizable contaminants for lightly contaminated air.
4. Catalyst activity appears to be maintained at water vapor concentrations that are typical of humidified indoor environments.

PCO of Gas-Phase Organic Compounds

Approximately 60 organic compounds have been studied in heterogeneous gas-phase PCO. Forty-three of the more salient organic compounds of concern in indoor environments are listed below along with published PCO scientific investigations of them.

1. 1,1,1-trichloroethane ($\text{CHCl}_2\text{CH}_2\text{Cl}$) – d’Hennezel & Ollis (1997), d’Hennezel (1998), Isidorov et al. (1997)
2. 1,3-butadiene ($\text{H}_2\text{C}:\text{CHHC}:\text{CH}_2$) – Obee & Brown (1995)
3. 1,4-dioxane ($\text{OCH}_2\text{CH}_2\text{OCH}_2\text{CH}_2$) – d’Hennezel and Ollis (1997), d’Hennezel (1998)
4. 1-butanol ($\text{CH}_3(\text{CH}_2)_3\text{OH}$) – Peral and Ollis (1992), Blake and Griffin (1988)
5. 1-butene (C_4H_8) – Cao et al. (1999)
6. 2-hexene (C_6H_{12}) – Ohno et al. (1998)
7. 2-propanol (isopropanol, $\text{C}_3\text{H}_8\text{O}$) – Ait-Ichou et al. (1985), Alberici and Jardim (1997), Bickley et al. (1973), Cunningham and Hodnett (1981), Larson et al. (1995), Ohko et al. (1997), Ohko et al. (1998a), Wentworth and Chen (1994)
8. acetaldehyde (CH_3CHO) – d’Hennezel & Ollis (1997), Obuchi et al. (1999), Ohko et al. (1998b), Sauer and Ollis (1996), Shifu et al. (1998), Sopyan et al. (1994), Sopyan et al. (1996a)
9. acetic acid ($\text{CH}_3\text{CO}_2\text{H}$) – Muggli and Falconer (1999), Sclafani et al. (1988)
10. acetone (CH_3COCH_3) – Alberici and Jardim (1997), Peral and Ollis (1992), Sauer and Ollis (1994), Shifu et al. (1998), Vorontsov et al. (1997b), Vorontsov et al. (1999), Yu et al. (1998), Zorn et al. (1999)
11. benzene (C_6H_6) – Atkinson and Schmann (1989), d’Hennezel and Ollis (1996), d’Hennezel and Ollis (1997), d’Hennezel et al. (1998), Einaga et al. (1999), Fu et al. (1995), Jacoby et al. (1996), Larson and Falconer (1997), Sauer et al. (1995), Seuwen and Warneck (1994), Sitkiewitz and Heller (1996)
12. butyraldehyde ($\text{CH}_3(\text{CH}_2)_2\text{CHO}$) – Peral and Ollis (1992)
13. carbon dioxide (CO_2) – Anpo et al. (1995) reported on the ‘reduction’ of CO_2
14. carbon monoxide (CO) – Anderson et al. (1996), Linsebigler et al. (1996b), Vorontsov et al. (1997a, 1998b)
15. chloroform (CHCl_3) – Alberici and Jardim (1997), Alberici et al. (1998)
16. dichloromethane (CH_2Cl_2) – Alberici et al. (1998)
17. diethyl ether ($(\text{C}_2\text{H}_5)_2\text{O}$) – Vorontsov et al. (1997b)
18. dimethoxymethane ($\text{C}_3\text{H}_8\text{O}_2$) – Alberici and Jardim (1997)
19. dimethylmethylphosphonate (DMMP, $(\text{CH}_3)_2\text{CH}_3\text{PO}_2$) – Obee and Satyapal (1998)
20. ethanol ($\text{C}_2\text{H}_5\text{OH}$) – Cunningham et al. (1974), Kennedy and Datye (1998), Muggli et al. (1996), Muggli et al. (1998), Nimlos et al. (1996), Sauer and Ollis (1996), Vorontsov et al. (1997b)
21. ethylene ($\text{H}_2\text{C}:\text{CH}_2$) – Fu et al. (1996a), Obee and Hay (1997), Sirisuk et al. (1999), Yamazaki et al. (1999), Zorn et al. (2000)
22. formaldehyde (HCHO) – Noguchi et al. (1998), Obee (1996), Obee & Brown (1995), Peral & Ollis (1992)
23. iso-octane ($(\text{CH}_3)_2\text{CH}(\text{CH}_2)_4\text{CH}_3$) – Alberici and Jardim (1997)
24. isopropyl alcohol (IPA, $(\text{CH}_3)_2\text{CHOH}$) – Brinkley & Engel (1998a); Brinkley & Engel (1998b)
25. isopropylbenzene (C_9H_{12}) – Alberici and Jardim (1997)
26. methane (CH_4) – Dreyer et al. (1997), Okabe et al. (1997)
27. methanol (MeOH , CH_3OH) – Alberici and Jardim (1997), d’Hennezel & Ollis (1997), Liu et al. (1985)
28. methyl acrylate ($\text{CH}_2:\text{CHCOOCH}_3$) – d’Hennezel & Ollis (1997)
29. methyl chloroform ($\text{C}_2\text{H}_3\text{Cl}_3$) – Alberici and Jardim (1997)

30. methyl ethyl ketone (MEK, $\text{CH}_3\text{COCH}_2\text{CH}_3$) – Alberici and Jardim (1997), d’Hennezel & Ollis (1997)
 31. methyl isopropyl ketone ($\text{C}_5\text{H}_{10}\text{O}$) – Alberici and Jardim (1997)
 32. methyl tert-butyl ether (MTBE, $(\text{CH}_3)_3\text{COCH}$) – d’Hennezel & Ollis (1997)
 33. methylene chloride (CH_2Cl_2) – Alberici and Jardim (1997), d’Hennezel & Ollis (1997)
 34. *m*-xylene (C_8H_{10}) – Peral and Ollis (1992)
 35. propene (C_3H_6) – Pichat et al. (1979)
 36. propionaldehyde ($\text{C}_2\text{H}_5\text{CHO}$)– Takeda et al. (1995), Takeda et al. (1997)
 37. pyridine ($\text{C}_5\text{H}_5\text{N}$) – Alberici and Jardim (1997), Sampath et al. (1994)
 38. *t*-butyl methyl ether ($\text{C}_5\text{H}_{12}\text{O}$) – Alberici and Jardim (1997)
 39. tetrachloroethylene (PCE, $\text{Cl}_2\text{C}:\text{CCl}_2$) – Alberici et al. (1998), Alberici and Jardim (1997), Hung & Yuan (1998), Li et al. (1998), Yamazaki-Nishida et al. (1996)
 40. toluene ($\text{C}_6\text{H}_5\text{CH}_3$) – Blanco et al. (1996), d’Hennezel et al. (1998), Ibrahim and de Lasa (1999), Ibusuki and Takeuchi (1986), Li et al. (1998), Luo and Ollis (1996), Méndez-Román & Cardona-Martínez (1998), Obee (1996), Obee & Brown (1995)
 41. trichloroethylene (TCE, $\text{CHCl}:\text{CCl}_2$) – Alberici et al. (1998), Alberici and Jardim (1997), Anderson et al. (1993), Annapragada et al. (1997), Buechler et al. (1999), Driessen and Grassian (1998), Driessen et al. (1998a, 1998b), Dibble and Raupp (1990), Dibble and Raupp (1992), Hung and Mariñas (1997a, 1997b), Hwang et al. (1998), Jacoby et al. (1994), Kim et al. (1996), Kim et al. (1998), Liu et al. (1997), Luo and Ollis (1996), Nimlos et al. (1993), Phillips and Raupp (1992), Wang et al. (1998a, 1998b, 1998c), Yamazaki-Nishida et al. (1993), Yamazaki-Nishida et al. (1995)
 42. vinyl acetate ($\text{CH}_3\text{COOCH}:\text{CH}_2$) – d’Hennezel & Ollis (1997)
 43. xylene (C_8H_{10}) –Blanco et al. (1996), d’Hennezel and Ollis (1997)
- Other - investigations of multiple VOCs – Lichtin et al. (1996), Obee and Hay (1999)

Table 1 lists some organic compounds that have been studied in photocatalysis.

PCO of Select Organic Compounds

Formaldehyde and Acetaldehyde. Noguchi et al. (1998) investigated the photocatalytic degradation of gaseous formaldehyde and acetaldehyde using a TiO_2 thin-film photocatalyst. The TiO_2 thin film was placed on soda lime glass and prepared from an STS-21 suspension (40 wt% anatase TiO_2 , pH 8.5, 20-nm particle diameter, $50 \text{ m}^2 \text{ g}^{-1}$ surface area) by the spin coating method. After spin coating, the film was calcined at 450°C for 1 h. The thickness of the translucent anatase TiO_2 film was $1.7 \mu\text{m}$. UV light was provided by a Hg-Xe lamp (Hayashi Tokei, Luminar Ace 210) and passed through a 365-nm band-pass filter. UV light intensity on the film surface was 1 mW cm^{-2} . Experiments were conducted at room temperature (22°C) and a relative humidity of 40%. Reactant concentration was between 30 and 2000 ppmv (parts per million by volume). Decomposition was initiated by UV illumination of TiO_2 film. No traces of formaldehyde in the reactor were observed after 80 min of reaction. The expected stoichiometric

CO₂ concentration was generated. The Langmuir-Hinshelwood (L-H) model provided the quantitative kinetics for the rate of the unimolecular surface reaction. The surface rate constant, k , values were 0.19 and 0.16 $\mu\text{mol min}^{-1}$ and the apparent adsorption coefficient, K_{app} , values were 0.51 and 0.21 $\mu\text{mol dm}^{-3}$ for formaldehyde and acetaldehyde, respectively. These results suggest little difference in the k values that directly correspond to the reactivity of each compound. However, the K_{app} values, which are related to the adsorption strength of each compound onto TiO₂, are significantly different – formaldehyde affinity for TiO₂ surface sites was ca. 2.5 times larger than that of acetaldehyde. This suggests that the differences in decomposition rates can be attributed, in part, to the differences in adsorption strength. Here, in the low reactant concentration region, the reaction kinetics are mass transfer limited.

PCO of Select Gas-Phase Inorganic Compounds

In contrast to the number of heterogeneous PCO investigations with organic compounds, only a few inorganic gas-phase compounds have been studied with PCO. These studies include:

1. ammonia (NH₃) – Mozzanega et al. (1979), Toshiaki et al. (1997), Toshiaki et al. (1998a, 1998b), Cant and Cole (1992)
2. hydrogen sulfide (H₂S) – Canela et al. (1998)
3. nitrogen oxides (NO_x, N₂O) – Anpo et al. (1991), Anpo et al. (1997), Hoshi et al. (1998), Ichihashi et al. (1997), Kudo and Nagayoshi (1998), Murata et al. (1998), Nishikata (1997), Wang et al. (1997), Cant and Cole (1992)
4. ozone (O₃) – Ohtani et al. (1992), Ohtani et al. (1993)
5. sulfur oxides (SO_x) – Fukumori (1998)

Catalyst Formulations

The nature of a photocatalyst is also important in determining the rate and efficiency of PCO. The anatase form of titanium dioxide has the desirable properties of being chemically stable, readily available, and active as a catalyst for photo-oxidation processes. The 3.2 eV band gap of TiO₂ matches the output of a wide variety of readily available artificial light sources or lamps. The photon efficiency of TiO₂ for reaction of hazardous molecules is generally rather low (~5%). Considerable work has been directed toward modifying TiO₂ and testing other semiconductors to identify methods to increase process

efficiency and to improve the overlap of the absorption spectrum of the photocatalyst with the solar spectrum. Various types of photocatalysts are discussed below.

Titanium Dioxide. Titanium dioxide (TiO_2 or titania) and modified forms, including different commercially available forms, heat treated materials, and materials prepared by a range of techniques including sol-gel chemistry (Negishi et al. 1995, Saitoh & Fukayama 1996, Zorn et al. 2000) and other methods (Sopyan et al. 1996b) comprise the vast majority of photocatalyst knowledge. Titania is largely obtained by either purchasing commercially available powder forms or by synthesis using sol-gel chemistry or flame formation techniques. Results from one investigation suggest a much higher rate of carbon dioxide formation with the sol-gel-derived form versus that obtained with the commercially available forms (Kominami et al. 2000). Sopyan et al. (1996a) reported higher photocatalytic activity for a UV-illuminated TiO_2 thin film vs. a TiO_2 powder form, as indicated by high total quantum yields. The higher activity of the sol-gel-derived form of TiO_2 photocatalysts is attributed to their high crystallinity and large surface area. Titanium dioxide is also one of the most stable photocatalysts because it does not photo-corrode, as does CdS.

Metal and Metal Ion Doping of Metal and Mixed-Metal Oxides. Metal ions have been introduced into the titanium dioxide lattice to modify the properties as presented in the following articles – Al (Muradov et al. 1996), Ga (Vergnon et al. 1978), Nb (Vergnon et al. 1978), and W (Muradov et al. 1996). Noble metals, primarily platinum, have been deposited onto the surface of titanium dioxide to enhance catalytic activity (Courbon et al. 1981, Courbon et al. 1984, Courbon et al. 1985, Fu et al. 1995, Linsebigler et al. 1996a).

Table 2 contains a list of some formulations for a photocatalyst. A large percentage of reported investigations use commercially available forms of particulate catalyst. In some cases, the particulate catalysts are used directly (e.g., fixed- or fluidized-bed reactors). Often the particulate catalyst is dispersed in a liquid and then deposited onto supports – metal, ceramics, monoliths, glass, among others – as a thin film with a thickness varying between 0.1 and 2 μm , and sometimes thicker. Other investigators (Zorn et al. 2000) employ sol-gel chemistry to synthesize materials that contain metal oxides as primary

particles (2-10 nm in size) suspended in water or alcohol. Thereafter the suspensions can be deposited onto supports via spin-coating, dip-coating, or spraying techniques. A wide variety of other semiconductors and other materials have been tested for photocatalytic activity including

Al₂O₃ (alumina), Fe₂O₃ – Casado et al. (1990)

V₂O₅, ZnO, ZrO₂ (zirconia), SnO₂, Sb₂O₄, CeO₂, WO₃ – Herrmann et al. (1981), Pichat et al. (1979)

Sn/SbO₂ – Pichat et al. (1979)

Poly (p-phenylene) – Toth et al. (1995)

SiO₂/TiO₂ and ZrO₂/TiO₂ – Fu et al. (1996c)

Supported Photocatalysts

Most experimental work in gas-phase photocatalysis is conducted with the photocatalyst deposited onto appropriate materials called *supports*. Titanium dioxide has been supported by a variety of surfaces including

glass (including fibers) – Kim et al. (1996), Trivedik (1994), Zorn et al. (2000)

glass rings – Zorn et al. (1999), Zorn et al. (2000), Sirisuk (2003)

silica (SiO₂) – Mune et al. (1996), Sauer and Ollis (1996), Takeda et al. (1995)

polymer – Takeuchi (1996)

thin films – Kim et al. (1996), Negishi et al. (1995), Saitoh and Fukayama (1996)

zeolite, alumina – Takeda et al. (1995)

carbon – Takeda et al. (1995), Ishihara and Furutsuka (1996)

paper – Matsubara et al. (1995)

metal oxides and ceramics – Sauer and Ollis (1996), Takeuchi (1996)

PCO Conversion and Mechanisms

Extent of Oxidation. Alberici and Jardim (1997) investigated the gas-phase photocatalytic destruction of 17 VOCs over illuminated TiO₂ under plug-flow reactor conditions of 200 ml min⁻¹ flow rate, 23% relative humidity, 21% oxygen and an organic compound concentration range of 400-600 ppmv. At steady state, high conversion yields were obtained for trichloroethylene (99.9%), isooctane (98.9%), acetone (98.5%), methanol (97.9%), methyl ethyl ketone (97.1%), t-butyl methyl ether (96.1%), dimethoxymethane (93.9%), methylene chloride (90.4%), methyl isopropyl ketone (88.5%), isopropanol (79.7%), chloroform (69.5%) and tetrachloroethylene (66.6%). Unfortunately, the photodegradation of isopropylbenzene (30.3%), methyl chloroform (20.5%) and pyridine (15.8%) was not particularly

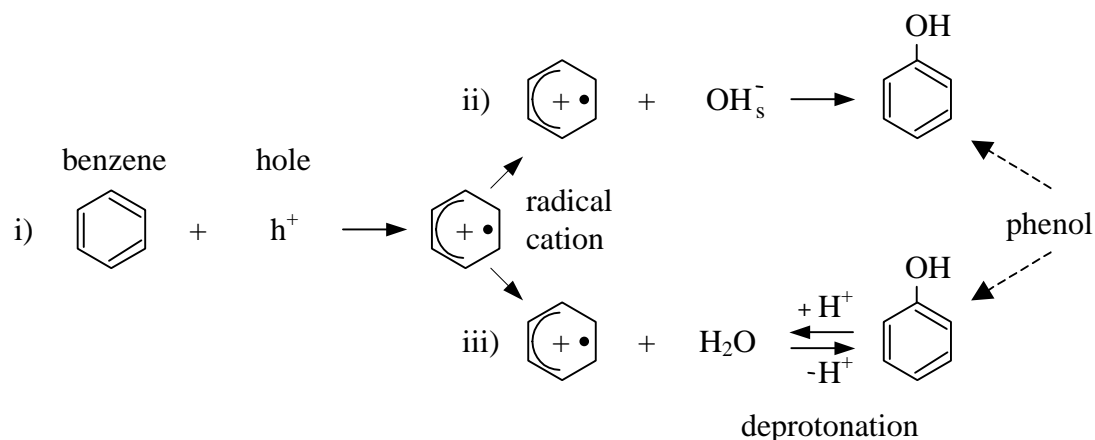
efficient. However, total conversion (i.e., removal of target reactant species) was achieved for all 17 compounds tested, either through multiple reactor passes or longer residence times for a single pass reactor.

Reaction Mechanisms. Numerous individual reactions are involved in this 3-step process – initiation, propagation and termination – which results in rather complex reaction mechanisms being proposed. Examples of some key conclusions of reaction mechanism studies are provided below.

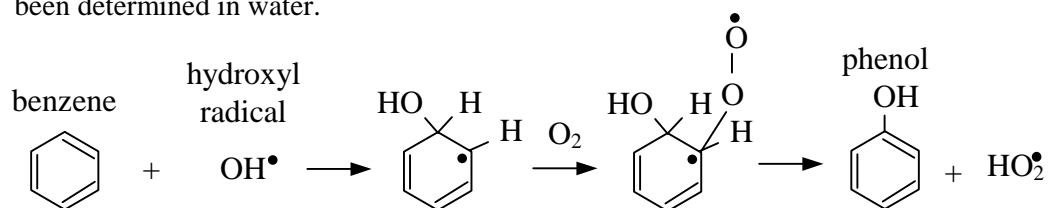
Toluene. The benzyl radical is suggested as the key species that leads to formation of benzyl alcohol and benzaldehyde (Blanco et al. 1996, Sitkiewitz & Heller 1996). Toluene degradation rate is enhanced by the simultaneous presence and degradation of trichloroethylene (TCE); the increased rate is assumed to be due to the formation of active chlorine radicals (d’Hennezel and Ollis 1997). Prechlorination of the TiO₂ surface by use of aqueous HCl is shown to enhance the toluene reaction rate; it is proposed that Ti/Cl⁻ surface species can trap photogenerated holes and degrade some organic pollutants through the production of chlorine radicals (d’Hennezel 1998).

Benzene. It has been shown that benzene is less susceptible to photocatalytic oxidation than toluene (d’Hennezel & Ollis 1997). Wallington et al. (1988) have studied chlorine radical and hydroxyl radical reactivities with toluene and benzene and found that toluene is 13 times more reactive than benzene with chlorine radicals, but much closer reactivities between toluene and benzene are observed with only hydroxyl radicals present. The difference could partially explain why the presence of chlorine does not enhance the degradation rate of benzene (d’Hennezel et al. 1998). d’Hennezel et al. (1998) have proposed two routes for benzene degradation:

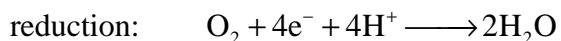
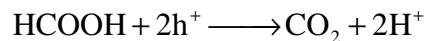
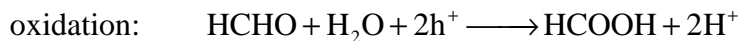
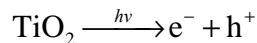
1. (i) Direct hole oxidation followed by reaction of the resulting radical cation either
 - (ii) with a surface basic OH group, or
 - (iii) with an adsorbed water molecule and subsequent deprotonationto yield phenol, the major intermediate detected.



2. OH^\bullet radical addition to yield a cyclohexadienyl radical. Addition of oxygen to this radical and elimination of the radical HO_2^\bullet produces phenol by analogy with what has been determined in water.



Formaldehyde. Noguchi et al. (1998) investigated the photocatalytic degradation of gaseous formaldehyde (and acetaldehyde) using a TiO_2 thin film photocatalyst. Although CO_2 is the final oxidation product, intermediates and/or byproducts were extracted from the TiO_2 surface. After 75% of the formaldehyde reacted, the product distribution was CO_2 (80%) as a gas and formic acid ($HCOOH$) (20%), which remained on the surface as a partial oxidation byproduct. Similarly for PCO of acetaldehyde, the product distribution was CO_2 (50%) as a gas and $HCOOH$ (20%), acetic acid (CH_3COOH) (25%) and other species (5%) as partial oxidation byproducts. With prolonged UV illumination, all the intermediates and byproducts were oxidized to CO_2 . Peral and Ollis (1992) and Aguado et al. (1994) have described the major oxidative and reductive processes in the photodegradation of formaldehyde. The process can be written as



Competitive Adsorption

It is recognized that there will be several gaseous contaminants present in indoor air environments. Successfully treating all or nearly all these contaminants with PCO reactors will require knowledge of the *competitive adsorption* process. That is, each contaminant, in addition to water and oxygen, in a mixture of several gas-phase species will have its own affinity for adsorption to sites on a photocatalytic surface. Obee and Brown (1995) and Obee and Hay (1999) have studied the competitive adsorption of compounds on the surface of a photocatalyst. Recall the aforementioned study of Noguchi et al. (1998) where the larger affinity of formaldehyde for TiO_2 surface sites over that of acetaldehyde resulted in higher reaction rates for formaldehyde, suggesting that the differences in decomposition rates can be attributed, in part, to the differences in adsorption strength.

Reactor Design

Several articles address topics relevant to the design of reactors for photocatalytic processes including non-concentrating reactors (Takeuchi 1995), kinetic modeling (Sauer and Ollis 1996), ceramic monoliths (Sauer and Ollis 1996), and field tests (Ren et al. 1995). In recent years, successful laboratory demonstration of heterogeneous PCO for processing waste streams of gas contaminants has resulted in industrial interest. There are several configurations of gas-solid heterogeneous PCO reactors; a few are presented here.

Supported Powder Layer. A feed stream of gas is passed vertically downward through a powdered photocatalyst supported on a porous glass frit, which is illuminated from above (Fig. 2). The reaction rate is reported to increase linearly with the thickness of powder layer (0 mm - 4 mm) and is independent of

catalyst depth greater than 4.5 mm, presumably corresponding to complete photon absorption (Courbon et al. 1973). The powder layer reactor was employed in the early studies of Teichner's group. Other investigators [Blake and Griffin (1988), Dibble and Raupp (1990), Peral et al. (1992), and Peral et al. (1997)] have also employed this design.

Annular. A light source located along the centerline illuminates the catalyst-filled reactor (Fig. 3). In studies with acetone it was observed that at low catalyst loading the reaction rate decreases because of insufficient catalyst to capture all the light, while with high loadings of catalyst high concentrations lead to excessive opacity. In the latter case, the rate began to diminish because an increasing fraction of the reactor flow is operating with insufficient or no light (Peral et al. 1997).

Fluidized Bed. Fluidized bed reactors pass a gas feed stream vertically through a transparent container filled with catalyst (Fig. 4), promoting mixing between the gas and catalyst particles. Illumination is from the side and there is a particle disengagement section near the top. Bench-scale laboratory studies with fluidized bed photoreactors have been investigated for ammonia oxidation (Cant and Cole 1992) and photocatalytic destruction of trichloroethylene (TCE) in humidified air (Dibble and Raupp 1992). In the latter study, catalysts suitable for fluidization were prepared via sol-gel impregnation of silica gel (0-63 g TiO_2/g silica gel) of 250-450 nm diameter. The apparent quantum efficiencies were reported between 2 and 8%, with a maximum of 13%. Dibble and Raupp (1992) cite advantages of the fluidized bed configuration to include excellent reactant-catalyst contacting, high volumetric flow rates, and low pressure drop, the latter attribute being exceedingly important in applications of high throughput.

Honeycomb Monolith. The honeycomb monolith provides a low-pressure drop catalyst configuration, typically providing pressure drops that are much lower than those associated with packed or fluidized beds (Peral et al. 1997). One challenge for the monolith photoreactor design is providing sufficient illumination to the catalyst. Some practitioners employ end-on illumination (Suzuki et al. 1991). Observations from studies with a photocatalytic monolith for oxidation of odors demonstrated that the kinetics of disappearance of each of several odor compounds was nearly first order (Suzuki et al. 1991). Sauer and Ollis (1994) confirmed the observations of Suzuki's group using an illuminated TiO_2 -coated

monolith, where reactor performance for the oxidation of acetone was modeled sufficiently with Langmuir-Hinshelwood kinetics. Later, Luo and Ollis (1996) analyzed the behavior of the photocatalytic monolith including the influence of various flow regimes – developing (entrance region), undeveloped, and developed – on reactor performance. Using rate parameters for various oxygenates, it appears that appreciable conversions occur for small channel Reynolds numbers (1-50); single channel experiments support the analysis (Luo and Ollis 1996).

Other configurations. Since photocatalyst prepared either from sol-gel chemistry or as suspensions of powders can be deposited on a variety of surfaces, many other photoreactor geometries and configurations are possible. The liquid-solid photocatalysis literature cites the application of immobilized photocatalyst on fiberglass mesh, glass beads which are solid (for packed beds) or hollow (for oil slick treatment), coiled glass tubes (for total organic carbon analyzers), and within pillared clays and zeolites. Catalyst-coated optical fibers for liquid or gas treatment have been analyzed (Marinangeli and Ollis 1977, Marinangeli and Ollis 1980, Marinangeli and Ollis 1982). Aguado et al. (1992) describe an experimental device to conduct solid-liquid-gas photocatalytic studies. Discussion would not be complete without mentioning the ubiquitous packed-bed design wherein photocatalyst is packed around light sources within a reactor housing or shell. (NOTE: The packed-bed design can be thought of as an annular design.) To date, companies that are commercializing PCO technology for gas-phase applications have generally adapted the packed-bed design.

Ibrahim and de Lasa (1999) investigated the photocatalytic conversion of toluene in a newly designed batch photoreactor, in which TiO_2 is supported on a filter mesh with good contact with near UV light, TiO_2 , and air. The photoreactor is designed with special features including a Venturi section and a heated perforated plate. The heated perforated plate minimizes water adsorption on the mesh and consequently water effects on the reaction rate. The system performance is examined for different toluene concentrations and two humidity levels. Apparent quantum yields were estimated to be in many cases greater than 100% and as high as 450%.

Light Sources and Irradiance

Activating a photocatalyst requires energy from a light source that is greater than the band-gap. Some suitable light sources are listed in Table 3. For example, Noguchi et al. (1998) employed UV light provided by a Hg-Xe lamp and passed through a 365-nm band-pass filter. UV light irradiance on the film surface was 1 mW cm^{-2} . Fluorescent light sources with the energy needed to activate photocatalysts are those that emit predominantly in the near-UV or UVA (320-400 nm). Light sources and the electronic and magnetic ballasts that power them are practical for use in commercial-scale PCO reactors. Here, the so-called *black light* (or “BL”) and black light blue (or “BLB”) lamps, which are designed to emit in the UVA spectrum, can find application. One can expect that the irradiance (mW cm^{-2}) emitted from a light source will diminish with illumination time. Indeed, manufacturers of fluorescent light sources often rate a useful life varying between 5,000 and 10,000 h. During the continuous operation of a hot-cathode (i.e., low-pressure Hg vapor lamp) fluorescent light source, the gradual thinning of the tungsten filament can lead to complete failure of the bulb. The decrease in light irradiance with illumination time will affect the performance of photocatalytic reactors. The plots in Fig. 5 reveal approximately a 50% decrease in light irradiance after 3000 hours ($\sim 1/3$ year for continuous operation) of illumination.

In general, the rates of photocatalytic reactions depend on the light irradiance. For illumination by a UV source at irradiances in excess of one sun equivalent, reaction rates increase in proportion to the square root of the irradiance. For irradiances below one sun equivalent, reaction rates increase approximately linearly with the irradiance (Obee and Brown, 1995). One sun equivalent is defined at $4.1 \times 10^{15} \text{ photons cm}^{-2} \text{ s}^{-1}$ for photons with wavelengths shorter than 385 nm (Raupp and Junio, 1993). A linear dependence was observed between irradiance and the rate of photocatalytic oxidation of ethylene over titania pellets (Yamazaki et al. 1999) and in the photocatalytic decomposition of gaseous 2-propanol (Ohko et al. 1997).

The square root dependence of the reaction rate arises as a consequence of the enhanced rate of recombination of photogenerated electrons and holes that occurs when the photocatalyst is subjected to high irradiance UV light (Hoffmann et al., 1995). Aguado et al. (1994) reported that the photocatalytic degradation of formic acid over certain types of titania membranes obeys a square root dependence on

light irradiance. Mills and Morris (1993) studied the photomineralization of 4-chlorophenol and reported that the reaction rate is dependent on $I^{0.74}$, a power dependence that lies in the transition region between the exponents expected at low irradiance ($I^{0.5}$) and high irradiance (I^1).

Catalyst Life/Fouling

It has been reported that photocatalysts can be fouled and poisoned or deactivated thereby decreasing their performance (Table 4). For example, during the PCO of toluene and benzene, a yellow discoloration of the catalyst surface was observed with the gradual deactivation of the catalyst (d'Hennezel et al. 1998). It has been shown that toluene oxidizes rapidly over UV-irradiated TiO_2 to form intermediate products that are strongly adsorbed and much less reactive than toluene (Larson and Falconer 1997). This study also demonstrated that benzaldehyde and benzyl alcohol react 10-30 times faster than toluene. That observation prompted the investigators to conclude that these compounds are not likely to be the stable intermediate products formed during PCO of toluene (Larson and Falconer 1997). Therefore, these authors postulated that the unidentified yellow material recovered from used TiO_2 could result from adsorption of less reactive intermediates (Larson and Falconer 1997). A yellowish discoloration of TiO_2 during PCO is mentioned by several investigators both for toluene (Ibusuki and Takeuchi 1986, Larson and Falconer 1997) and for benzene (Fu et al. 1995, Jacoby et al. 1996, Sitkiewitz and Heller 1996). In another study (Wolfrum et al. 1997) it was demonstrated that hexmethylidisilazane (HMDS) rapidly deactivated a catalyst. In another PCO study with toluene, Alberici and Jardim (1997) detected catalyst (TiO_2) deactivation when the reactor was operated under steady-state plug-flow reaction conditions of 200 ml min^{-1} , 23% relative humidity, 21% oxygen, and a toluene concentration range between 400 and 600 ppmv. However, illuminating the catalyst in the presence of hydrogen peroxide restored the catalyst activity.

Muggli et al. (1988) identified the concentrations of species on a TiO_2 surface during photocatalytic oxidation (PCO) of ethanol. Ethanol and its partial oxidation intermediates (acetaldehyde, acetic acid, formaldehyde, and formic acid) were reported to be on the catalyst surface, and their concentrations depended on the feed concentrations of ethanol, O_2 , and water. The rate of PCO was

greater initially than at steady state for all experimental conditions, and the initial deactivation was ascribed in part to the accumulation of acetaldehyde on the surface.

Effect of Water Vapor

Water vapor molecules compete with other feed stream gases, notably reactant species and molecular oxygen, for sites on the photocatalyst surface. The effect of water vapor in photocatalytic processes reported in several investigations is presented in Table 5. Summaries from selected PCO studies examining the effect of water vapor are described here.

Benzene. The presence of water vapor in a feed stream containing benzene enhances its PCO over TiO₂ (Table 5). High initial conversion followed by a decrease over time is observed for three different inlet water concentrations – 0, 1000, 8000 mg m⁻³ (0, 1342, 10,800 ppmv) – and conversion stabilized after 3 hr of reaction at 20%, 36%, and 40% conversion, respectively (d’Hennezel et al. 1998). Other investigations confirm the finding that the presence of water vapor is necessary for continued high benzene conversion (Fu et al. 1995, Sitkiewitz and Heller 1996).

***o*-xylene.** Ameen and Raupp (1999) reported that the reversible deactivation rate during gas-solid heterogeneous PCO of airborne dilute *o*-xylene over near-UV irradiated TiO₂ catalyst depended on *o*-xylene concentration and the relative humidity of the reactant stream. The deactivation decreased linearly with decreasing *o*-xylene concentration and increasing relative humidity. The concentration of *o*-xylene and aromatic partial oxidation intermediates on the titania surface are significantly higher for conditions of low relative humidity than for conditions of high humidity. Experiments performed at low relative humidity favored the buildup of *o*-xylene and *o*-toluic acid on the catalyst surface. Regeneration of the catalyst deactivated during the photocatalytic oxidation process operated at high humidity requires much shorter catalyst treatment time than for the catalyst deactivated by photocatalytic oxidation operated at low humidity. The observations of Ameen and Raupp (1999) suggest that hydroxyl radicals play a significant role in both the oxidation and the regeneration processes.

Trichloroethylene (TCE). Annapragada et al. (1997) studied the gas-solid heterogeneous photocatalytic oxidation of TCE in humid airstreams in a bench-scale annular photocatalytic reactor operated under

partial vacuum. Reduction of the operating pressure at fixed feed conditions and molar feed rate significantly enhanced PCO performance as measured by the observed TCE conversion. Higher conversions were obtained in spite of a reduction in the residence time accompanying the lower pressure operation. The greatest enhancements in the TCE destruction efficiency occurred for low TCE feed concentrations and high water vapor levels. The performance enhancement appears to be linked to reduction in the absolute water vapor concentration and competition between TCE and water vapor for adsorption sites on the catalyst.

Formaldehyde, toluene and 1,3-butadiene. Obee and Brown (1995) examined the effects of humidity and trace (sub-ppmv) contaminant levels on the oxidation rates of formaldehyde, toluene, and 1,3-butadiene. The evaluation also included variations in UV irradiance and flow residence time. Irradiances from inexpensive mercury fluorescent lamps vary between 1-10 mW cm⁻². The data indicated the reaction was first-order for the three reactants at the sub-ppmv level. An important finding was that competitive adsorption between water and trace (sub-ppmv) contaminants has a significant effect on the oxidation rate. The dependencies of humidity and contaminant concentrations on the oxidation rates are explained as resulting from competitive adsorption on available hydroxyl adsorption sites and on changes in hydroxyl radical concentrations.

Ethylene. Fu et al. (1996a) investigated the photocatalytic degradation of ethylene in airstreams over the temperature range 30-110°C using a packed bed reactor containing sol-gel-derived TiO₂ or platinumized TiO₂ particulates. Results from this study indicate that the reactivity of ethylene is enhanced with increasing temperature and that the fraction of ethylene that reacts is stoichiometrically oxidized to CO₂ under all operating conditions. The effect of raising the temperature has been ascribed to decreasing adsorption of water for both types of catalysts, as well as an increase in conventional heterogeneous catalytic reactions occurring on the Pt/TiO₂ catalyst. In addition, platinumizing the TiO₂ photocatalyst and increasing the content of water vapor in the gaseous feed streams both decrease the rate of photocatalytic

oxidation of ethylene. The activation energies for the photocatalytic and heterogeneous catalytic oxidation of ethylene were determined to be 13.9-16.0 kJ mol⁻¹ and 82.8 kJ mol⁻¹, respectively.

Reaction By-Products

Reactions with No By-product Formation. Under steady-state reaction conditions whereby titanium dioxide is illuminated in a plug flow reactor at 200 ml min⁻¹, 23% relative humidity, 21% oxygen, and an organic compound concentration range between 400 and 600 ppmv, Alberici and Jardim (1997) reported that no detectable by-products formed during the PCO of 17 VOCs – trichloroethylene, isooctane, acetone, methanol, methyl ethyl ketone, t-butyl methyl ether, dimethoxymethane, methylene chloride, methyl isopropyl ketone, isopropanol, chloroform, tetrachloroethylene, isopropylbenzene, methyl chloroform, pyridine, and carbon tetrachloride.

Reactions With By-product Formation. Alberici et al. (1998) utilized on-line mass spectrometry to monitor and identify the by-products and total mineralization products of TiO₂/UV photocatalytic degradation of four chlorinated volatile organic compounds (VOCs) including trichloroethylene (TCE), tetrachloroethylene (PCE), chloroform, and dichloromethane. Several by-products were detected including phosgene for TCE, PCE, and chloroform; dichloroacetyl chloride for TCE; and trichloroacetyl chloride for PCE.

Other PCO-related Topics

Review articles provide a broad overview of various aspects related to the physics, chemistry, engineering, and application of photocatalysis. Review articles that cover broad topics mentioned here can be found in the following: solar processes (Takeuchi and Kutsuna 1996), disinfection (Murakami and Ishida 1996), indoor air quality (Murakami and Ishida 1996, Sugawara 1996, Takaoka and Ebihara 1995), and environmental applications (Takeuchi and Kutsuna 1996).

Numerous survey articles elaborate on the many issues comprising the principles and practice of PCO. Fu et al. (1996b) and Peral et al. (1997) review the application of heterogeneous photocatalysis for purification of air. Rao and Natarajan (1994) provide a review of the particulate models in heterogeneous

photocatalysis. Hoffmann et al. (1995) provides a review of the environmental applications of semiconductor photocatalysis. Linsebigler et al. (1995) discuss the principles, mechanisms and selected results of PCO.

As an aid to the more interested reader, a bibliography of scientific articles concerning research, development, and patents awarded in the application of heterogeneous photocatalysis for treating air and aqueous feed streams is compiled and periodically reported by the National Renewable Energy Laboratory (Blake 1999). This bibliography is a valued resource for end-users that desire a condensed summary of research articles in the field of heterogeneous photocatalysis.

Predictive Modeling – Contaminant Removal from a Zone

Although it is an intuitive and unproven assumption, scaling up the aforementioned bench-top laboratory reactors for commercial-scale applications of gas-solid photocatalysis may require conventional heterogeneous reactor configurations including fixed and fluidized beds, transport reactors, and monolith, among others. Whichever configuration is appropriate for a given application, the absolute reaction rate of contaminant removal must match the contaminant generation and infiltration rate minus the exfiltration rate. This requirement for efficient conversion processes must be balanced against designs that achieve low-pressure drop, a significant concern of PCO devices used for air purification in the office, home or factory. As such, it may be less important to achieve high reactant conversion/oxidation on single passes through a commercial scale PCO device than is typical for other chemical processing and in particular, dust removal technologies, where single-pass removal efficiencies can be high. Furthermore, because PCO reactors operated for purification will recycle air multiple times, the absolute level of conversion per pass through the reactor may be less important. Modeling the disappearance of a contaminant species via use of a photocatalytic reactor is introduced by describing the physical conditions of an enclosure containing a PCO reactor.

Physical Model. Consider an enclosure (building or residence) as a structure with porous walls. While the enclosure may have multiple zones, one can consider the enclosure as a single room or zone with

volume V_z . In the presence of a pressure differential between the ambient and the zone, there is movement of (ambient) outside air (gas) into the zone with a volumetric flow rate of v_i – called infiltration – and movement of the air from the zone to the ambient at the (same) rate of v_i – called exfiltration. Consider the scenario in which infiltration air is comprised of one (gaseous) contaminant A in the parts per million vapor (ppmv) range and the balance is air (N₂:O₂). The infiltrating contaminant has a concentration of C_{Ai} . Assuming the air in the zone is well mixed, the concentration of the contaminant in exfiltration air is C_A . Additionally, consider a source(s) in the enclosure that uniformly generates the contaminant in the zone at a rate of \dot{S}_A . Consider that the zone contains a PCO treatment device or reactor, which is small in relation to the size of the zone. The device has its own dedicated fan that forces zonal air through the device at a volumetric flow rate of v_R . The rate of disappearance of the contaminant from the air passing through the device is r_A and requires a mass of photocatalyst, W , and period of time, t , to effect this removal. The contaminant enters the device at C_A and leaves at C_{AeR} .

Numerical Model. A mathematical model can be employed to determine the time varying concentration of the contaminant in the zone. A molar balance on the zone is given as

$$C_{Ai}v_i + C_{AeR}v_R - C_Av_i - C_Av_R + \dot{S}_AV_z = V_z \frac{dC_A}{dt} \quad (1)$$

The steady-state molar balance on the reactor is given by

$$C_Av_R - C_{AeR}v_R - r_AW = 0 \quad (2)$$

Kinetic Modeling of PCO Reactor

The kinetics of PCO reactions can be determined by performing experiments in which the reactors are operated in either of two modes – recirculation (batch) or plug-flow (single-pass). Both approaches are described here. A kinetic model is required to estimate the removal of a (contaminant) species by the treatment device. The fractional conversion, f_A , is calculated as

$$f_A = 1 - \frac{C_A}{C_{A0}} = 1 - \frac{P_A}{P_{A0}} = 1 - \frac{n_A}{n_{A0}} \quad (3)$$

where C_A is the concentration of the species of interest (reactant) at a given time during the reaction and C_{A0} is its initial concentration, P_A is the pressure of the reactant and P_{A0} is its initial pressure, and n_A are the moles of reactant and n_{A0} are its initial number of moles. Assuming ideal gas behavior, Equation 3 makes use of the partial pressure of the reactant as

$$P_A = \frac{n_A \cdot R \cdot T}{V} = \frac{n_{A0} \cdot R \cdot T \cdot (1 - f_A)}{V} = P_{A0} \cdot (1 - f_A) \quad (4)$$

where R is the gas constant, T is the absolute temperature, V is volume (assumed not to change depending on stoichiometry of the reaction).

Models based on power law rate expressions have also been reported to provide adequate approximation of kinetic data for photocatalytic reactions (Fu et al., 1996b; Fu et al., 1996c, Zorn et al., 1999). Models based on Langmuir-Hinshelwood rate expressions have been used successfully to fit kinetic data of photocatalytic reactions (Dibble and Raupp, 1990; Sabate et al., 1991; Peral and Ollis, 1992; Obee and Brown, 1995; Sauer and Ollis, 1996; Obee and Hay, 1997; Yamazaki et al, 1999; Zorn et al., 1999).

Recirculation (or Batch) Reactor Operation and Modeling. In one approach, PCO treatment devices are operated as recirculation or batch reactors. Here, the reactors are placed within a gas-tight chamber with volume V_{res} . The chamber is backfilled with a reactant gas with an overwhelming stoichiometric excess of oxygen (often air) as the balance. Then, a flow of reactant gases through the reactor is established. After a steady-state initial reactant gas concentration (C_{A0}) is established, an experiment is initiated ($t = 0$) by illuminating the light source(s). Sample volumes (\ll volume of the chamber) of the gasses in the chamber are taken periodically and analyzed with appropriate analytical instruments (e.g., GC/FID, GC/TCD, GC/MS, FTIR, PID, etc.). An experiment is terminated after a considerable amount of the reactant gas has reacted, i.e., $f_A > 0.9$. The concentration vs. time data obtained from the experiment is analyzed according to an appropriate kinetic model.

Power Law model. Assuming that the PCO of reactant species follows a power law model, the reactor design equation is (Edwards 1994)

$$-r_A = k_A C_A^n = \frac{-V_{res}}{W} \frac{dC_A}{dt} \quad (5)$$

In Eq. 5, $-r_A$ is the rate of disappearance of species A, k_A is the reaction rate constant, and n is the reaction order. [Since the concentration of reactant gas occupying V_{res} decreases with reaction time, the term $\frac{dC_A}{dt}$ is negative. Therefore, a negative sign is required on the right-hand-side of Eq. 5.] Separating

variables and integrating solves Eq. 5 –

$$\frac{k_A W}{V_{res}} \int_{t=0}^{t=t} dt = - \int_{C_{A0}}^{C_A} \frac{dC_A}{C_A^n} = - \int_{C_{A0}}^{C_A} C_A^{-n} dC_A \quad (6)$$

or, after rearranging

$$\int_{C_{A0}}^{C_A} C_A^{-n} dC_A = - \frac{k_A W}{V_{res}} t \quad (7)$$

Eq. 7 can be solved for $n = 1/2$ (1/2-order model) as follows

$$\int_{C_{A0}}^{C_A} C_A^{-1/2} dC_A = \frac{C_A^{1/2}}{1/2} \Big|_{C_{A0}}^{C_A} = C_A^{1/2} - C_{A0}^{1/2} = - \frac{k_A W}{2V_{res}} t \quad (8a)$$

$$C_A^{1/2} = - \frac{kW}{2V_{res}} t + C_{A0}^{1/2} \quad (8b)$$

Since Eq. 8b is in the form of $y = mx + b$, the slope of the line fitting the data can be used to find the reaction rate constant (k) for

$$k_A = - \frac{2 V_{res}}{W} \text{slope} \quad (9)$$

where k has units of $\text{mol}^{1/2} \text{L}^{1/2} \text{g}^{-1} \text{s}^{-1}$. Equation 7 can also be solved for other reaction orders (n) including 1, 3/2, and 2; the rate expression, reactor design equation, regression plots and reaction rate constants are summarized in Table 6a.

Langmuir-Hinshelwood (LH) model. Because PCO reactors involve interactions between the gas-phase contaminants and the surface of the photocatalyst, LH rate expressions can be expected to provide a very good approximation of the overall reaction kinetics. The LH models of photocatalytic reactions are based on a mechanism that involves a reactant adsorbed on the surface of a catalyst. A simple LH rate expression for a reaction that is first order with respect to the fraction of the surface covered by adsorbed species A (θ_A) can be written as

$$-r_A = k_A \theta_A = \frac{k_A K_A C_A}{1 + K_A C_A} \quad (10)$$

For this case, the rate constant k_A typically has units of $\text{mol g}^{-1} \text{s}^{-1}$. The adsorption equilibrium constant for adsorbate A (K_A) typically has the units of reciprocal concentration (e.g., l-mol^{-1}). Combining Equations 3 and 10 gives

$$-r_A = \frac{k_A K_A C_{A0} (1 - f_A)}{1 + K_A C_{A0} (1 - f_A)} \quad (11)$$

Substitution of this LH rate expression into the design equation (Eq. 5) and subsequent integration leads to the following equation.

$$\frac{\ln(1 - f_A)}{f_A} = \frac{-k_A K_A W}{V_{res}} \frac{t}{f_A} + K_A C_{A0} \quad (12)$$

Linear regression analysis of the data in the form of a plot of $\frac{\ln(1 - f_A)}{f_A}$ versus $\frac{t}{f_A}$ is employed to determine the slope and the intercept of the straight line that best fits the data. The initial estimates of the parameters of the LH model (k_A and K_A) can be calculated using the following equations:

$$k_A = \frac{-V_{res} C_{A0}}{W \cdot \text{intercept}} \cdot \text{slope} \quad (13a)$$

$$K_A = \frac{\text{intercept}}{C_{A0}} \quad (13b)$$

Plug-Flow Operation and Modeling. In another approach, PCO reactors are operated in plug flow where the reactant species make a single pass through the reactor. Here, the independent variable is often the molar flow rate and is varied by either holding the inlet concentration (C_{A0}) constant and varying the volumetric flow rate or vice versa. The dependent variable is the fractional conversion.

The power law kinetic models can arise as limiting forms of LH rate expressions. As above, each model type is described, together with the linear form of the model used to obtain initial estimates of the kinetic parameters. These models are summarized in Table 6b. Nonlinear regression analyses of the kinetic data can be performed using several different kinetic models for the rate term in the design equation.

Power Law model. Assuming that the photocatalytic oxidation of reactant species follows a power law model, the reactor design equation is (Hill 1977)

$$\frac{W}{F_{A0}} = \int_{f_{A,in}}^{f_{A,out}} \frac{df_A}{-r_A} \quad (14)$$

In Eq. 14, $-r_A$ is the rate of disappearance of species A, W is the mass of the catalyst, and F_{A0} is the molar flow rate of reactant A entering the reactor. For a kinetic model that is $1/2$ order in the limiting reactant, the rate expression is of the form

$$-r_A = k_A C_A^{1/2} = k_A C_{A0}^{1/2} \sqrt{1-f_A} \quad (15)$$

where k_A is the reaction rate constant (with typical units of $\text{mol}^{1/2} \cdot \text{l}^{1/2} \cdot \text{s}^{-1} \cdot \text{g}^{-1}$). When this rate expression is combined with the design equation, and the result integrated, one obtains the following expression.

$$\sqrt{1-f_A} = 1 - \frac{k_A C_{A0}^{1/2}}{2} \cdot \frac{W}{F_{A0}}, \quad (16)$$

where F_{A0} is the initial molar flow rate. The task at hand is to determine k_A . The initial estimate for k_A is obtained from the slope of a plot of $\sqrt{1-f_A}$ versus W/F_{A0} using linear regression analysis. The initial estimate of the parameter k_A is calculated using the following relation:

$$k_A = \frac{-2 \cdot \text{slope}}{C_{A0}^{1/2}} \quad (17)$$

Note that the initial estimate of k_A can then be used as a starting value of this parameter in a subsequent nonlinear regression analysis of the data based on this model. In a similar manner, the expressions for the rate expression, reactor design equation, and regression plot to estimate k_A for reactions that are 1st-, 3/2-, and 2nd-order can be determined; they are summarized in Table 6b.

Langmuir-Hinshelwood models. Combining Eq. 11 into Eq. 14 and subsequent integration and rearranging gives a reactor design equation of

$$\frac{f_A}{\ln(1-f_A)} = k_A \frac{W}{F_{A0} \ln(1-f_A)} + \frac{1}{K_A C_{A0}} \quad (18)$$

Linear regression analysis of the data in the form of a plot of $\frac{f_A}{\ln(1-f_A)}$ versus $\frac{W}{F_{A0} \ln(1-f_A)}$ is employed to determine the slope and the intercept of the straight line that best fits the data. The initial estimates of the parameters of the LH model (k_A and K_A) can be calculated using the following equations:

$$k_A = \text{slope} \quad (19a)$$

$$K_A = \frac{1}{C_{A0} \cdot \text{intercept}} \quad (19b)$$

It is possible to develop a rate expression form in which a reaction rate constant k_{A0} is independent of light irradiance. For example, Peral and Ollis (1992) employed a LH rate equation of the form

$$k'_A = k_{A0} \left(\frac{I}{I_0} \right)^\alpha, \quad (20)$$

which can be integrated using a plug flow model. Eq. 20 contains an intensity dependence power, α . Sirisuk (2003), among others, have performed experiments to estimate α .

Approximating the Size of a PCO Reactor Based on Quantum Yield

The quantum yield (ϕ) of forming a product species in a light-induced chemical reaction is the number of molecules formed for each quantum of radiation absorbed. Often ϕ cannot be measured accurately because of light reflection and scattering. This fact likely explains why ϕ is not reported in most studies of heterogeneous photocatalysis. Nonetheless, it is an important metric of performance and is useful for comparing reactors from various laboratories. Because the quantitative analysis of product formation can be difficult (due to adsorption of product species on reactor surfaces and photocatalytic surfaces), it is sometimes estimated from the amount of reactant that disappears. Therefore the quantum yield can be estimated by

$$\phi = \frac{\text{moles degraded}}{\text{absorbed light irradiance}} = \frac{-r_{A0}W}{r_s A_s} \quad (21)$$

where r_s is the conversion rate on the surface of the catalyst, A_s is the surface area, and the initial reaction rate is determined via

$$-r_{A0} = \frac{k_A K_A P_{A0}}{1 + K_A P_{A0}}. \quad (22)$$

Consider the case where one desires to approximate the size of a large (i.e., field-test or commercial-scale prototype) PCO reactor and one has available an estimate of ϕ based either on published data or on experiments with a bench-top (or small-scale) reactor that is configured and operated similarly to that of the desired prototype. Also, assume that an estimate of the average light irradiance \bar{I} on the surface of the catalyst is known, which would likely be obtained by measurement. Under these assumptions, estimating the surface (or reaction) conditions and the feed conditions can provide an estimate for A_s as shown here.

Surface (or reaction) conditions. The energy per photon is determined with

$$E = \frac{hc}{\lambda} \quad (23)$$

where h is Planck's constant, c is speed of light, and λ is the wavelength of the light source's peak emission. The photon flux Γ can be estimated by

$$\Gamma = \frac{\bar{I}}{E} \quad (24)$$

and the conversion rate on the surface of the catalyst is given by

$$r_s = \frac{\phi \cdot \Gamma}{N_A} \quad (25)$$

where N_A is Avogadro's number.

Feed conditions: Assuming ideal gas behavior, one can estimate the initial molar flow (F_{A0}) rate of species A with volumetric flow rate Q_f and initial concentration C_{A0} as

$$F_{A0} = Q_f C_{A0}. \quad (26)$$

The surface area of the reactor for complete removal of species A can be estimated by

$$A_s = F_{A0} / r_s \quad (27)$$

In contrast to this estimation approach, once the kinetic model for a particular photocatalytic reaction over a particular catalyst is known, the mathematical model describing the performance of the reactor can be developed; recall for example Eq. 18. The development of the model requires not only the proper kinetic model, but also a model for the distribution of light irradiance within the reactor.

CONCLUSION

Numerous scientific investigations have elucidated the operating conditions necessary to achieve complete mineralization of many organic compounds to final products of CO₂ and H₂O. These reactions are achieved with only minimal requirements – light sources, power supply, a stable photocatalyst and oxygen. Many of these reactions occur at or near room temperature and atmospheric pressure. The presence of water vapor has been shown to enhance reaction rates for many reactant gases, often

occurring due to the generation of surface hydroxyl radicals. Additional factors affecting reactor performance include light irradiance, the presence of species causing catalyst deactivation (e.g., species containing Si and N), and competitive adsorption between individual species within a mixture of reactant gases. L-H and power-law kinetic models have demonstrated acceptable predictions of laboratory data.

With regard to commercial-scale applications, the present challenge is to design photocatalytic treatment devices that have low pressure drop, make efficient use of light (i.e., achieve high and uniform light irradiances over the surface of a catalyst that provides high quantum efficiencies), and employ a stable catalyst that can be readily re-activated if it becomes deactivated.

With regard to research that can be conducted to further advance the state-of-the-art in gas-phase heterogeneous photocatalysis, the HVAC industry will benefit from efforts that

- (1) continue to examine the influence of water vapor on competitive adsorption processes occurring on photocatalytic surfaces. (Here, the industry will benefit if testing is conducted within the range of relative humidity found in building environments (40-70%.));
- (2) investigate low-level concentrations (ppmv and sub-ppmv) in the inlet feed streams, which are concentrations that are representative of indoor environments;
- (3) conduct investigations in which the inlet feed stream contains multiple reactants (VOCs);
- (4) report reaction rate constants (Here, the HVAC industry can benefit if studies generate reaction rate constants that are reported in the peer-reviewed literature.);
- (5) explore innovative approaches for getting light at the catalyst – this includes but is not limited to the studies in which waveguide technology is addressed; and
- (6) develop better photocatalysts that limit (or negate) by-product formation, enhance reaction rates, and increase the rate of target specie adsorption onto the catalyst surface.

The review of the literature suggests the eventual need to develop a standard method of test so that valid comparisons can be made on reported performance metrics of photocatalytic reactors. Presently gas-phase heterogeneous photocatalysis holds promise for penetrating niche markets.

ACKNOWLEDGEMENTS

The authors of this report would like to thank several individuals for their contributions. Prof. Michael Zorn of the Environmental Chemistry and Technology Program at the University of Wisconsin-Green Bay is recognized for his contributions to the photocatalytic studies within our research group during his post-doctoral visit to UW-Madison. Gratitude is extended to Prof. Charles Hill and Dr. Akawat Sirisuk of the UW-Madison for discussions pertaining to PCO reactor modeling. This project was supported through ASHRAE research project 1134-RP.

NOMENCLATURE

Variable	Description	Units
A_s	Surface area	m^2
c	speed of light (= $2.998 \times 10^8 \text{ m s}^{-1}$)	$m \text{ s}^{-1}$
C_A	concentration of (gas) species A in a zone and in exfiltration air	mol L^{-1}
C_{A0}	initial concentration of (gas) species A	mol L^{-1}
C_{AeR}	concentration of (gas) species A exiting reactor and entering the zone	mol L^{-1}
C_{Ai}	concentration of (gas) species A in infiltration air	mol L^{-1}
E	energy per photon	J photon^{-1}
E_g	band gap (energy)	eV
f_A	fractional conversion	dimensionless
F_{A0}	initial molar flow rate of species A	mol s^{-1}
h	Planck's constant (6.626×10^{-34})	J s photon^{-1}
<i>intercept</i>	intercept in regression plot	dependent on plot
I	irradiance	$\text{J s}^{-1} \text{ m}^{-2}$
I_0	initial irradiance	$\text{J s}^{-1} \text{ m}^{-2}$
\bar{I}	average light irradiance	$\text{J s}^{-1} \text{ m}^{-2}$
k_A	reaction rate constant of species A	dependent on n
k'_A	reaction rate constant (n -order model); independent of light irradiation; temperature-dependent	$\text{mol}^{(1-n)} \text{ L}^n \text{ cm}^{2a} \text{ mW}^{-a} \text{ g}^{-1} \text{ s}^{-1}$
K_A	equilibrium adsorption constant	Pa^{-1}
n	reaction order – based on power law model	dimensionless

n_A	moles of reactant species A	mol
n_{A0}	initial moles of reactant species A	mol
N_A	Avogadro's number (= 6.02×10^{23} molecules mol ⁻¹)	molecules mol ⁻¹
P_A	partial pressure of species A	Pa
P_{A0}	initial partial pressure of species A	Pa
Q_f	volumetric flow rate	L s ⁻¹
r_A	rate of disappearance of species A	mol s ⁻¹ g ⁻¹
r_{A0}	initial rate of disappearance of species A	mol s ⁻¹ g ⁻¹
r_S	rate of conversion on surface of catalyst	mol s ⁻¹ m ⁻²
R	gas constant	L Pa mol ⁻¹ K ⁻¹
<i>slope</i>	slope of regression plot	dependent on plot
\dot{S}_A	generation rate of (gas) species A	mol s ⁻¹ L ⁻¹
t	time	s
T	temperature	K
V	volume occupied by reactant species	L
V_{res}	volume of gas-tight reservoir in batch reactor operation	L
V_z	volume of zone	L
W	mass of photocatalyst	g

Greek Symbols

α	exponent of light dependence parameter	dimensionless
ϕ	quantum yield	dimensionless
λ	wavelength of light	m
v_i	volumetric flow rate of infiltration air (outside air) into zone	L s ⁻¹

v_R	volumetric flow rate of gas through PCO reactor	$L s^{-1}$
ν	frequency of light	Hz
θ_A	surface coverage parameter	dimensionless
Γ	photon flux	$mol s^{-1} m^{-2}$

REFERENCES

- Aguado, M.A., J. Gimenez, and S. Cervera-March. 1992. A new continuous device to perform S-L-G photocatalytic studies. *Solar Energy* 49(1):47-52.
- Aguado, M.A., M.A. Anderson, and C.G. Jr. Hill. 1994. Influence of light intensity and membrane properties on the photocatalytic degradation of formic acid over TiO₂ ceramic membranes. *J. Molec. Catal.* 89(1-2):165-178.
- Ait-Ichou, I., M. Formenti, B. Pommier, and S.J. Teichner. 1985. *J. Catal.* 91:293-307.
- Alberici, R.M. and W.E. Jardim. 1997. Photocatalytic destruction of VOCs in the gas-phase using titanium dioxide. *Appl. Catal. B-Environ.* 14(1-2):55-68.
- Alberici, R.M., M.A. Mendes, W.F. Jardim, and M.N. Eberlin. 1998. Mass spectrometry on-line monitoring and MS2 product characterization of TiO₂/UV photocatalytic degradation of chlorinated volatile organic compounds. *J. American Soc. For Mass Spectrometry* 9(12):1321-1327.
- Alpert, D.J., J.L. Sprung, J.E. Pacheco, M.R. Praitie, H.E. Reilley, T.A. Milne, and M.R. Nimlos. 1991. *Sol. Energy Mater.* 24:594
- Ameen, M.M. and G.B. Raupp. 1999. Reversible catalyst deactivation in the photocatalytic oxidation of dilute *o*-xylene in air. *J. Catal.* 184(1):112-122.
- Anderson, M. A., S. Yamazaki-Nishida, and S. Carvera-March. 1993. Photodegradation of trichloroethylene in the gas phase using TiO₂ porous ceramic membrane. In D.F. Ollis and H. Al-Ekabi (eds.), *Photocatalytic purification and treatment of water and air*. Elsevier, Amsterdam. 405-420.
- Anderson, M. A., W.A. Zeltner, X. Fu, D.T. Tompkins, and D.T. Reindl. 1996. Photocatalytic degradation of formaldehyde and other VOCs in indoor air. *CIAR Currents*. December.
- Annapragada, R., R. Leet, R. Changrani, and G.B. Raupp. 1997. Vacuum photocatalytic oxidation of trichloroethylene. *Environ Sci. Technol.* 31(7):1898-1901.
- Anpo, M., H. Yamashita, Y. Ichihashi, and S. Ehara. 1995. Photocatalytic reduction of CO₂ with H₂O on various titanium-oxide catalysts. *J. Electroanalytical Chem.* 396(1-2):21-26.
- Anpo, M., T. Nomura, T. Kitao, E. Giamello, D. Murphy, M. Che, and M.A. Fox. 1991. Approach to denox-ing photocatalysis. 2. Excited-state of copper ions supported on silica and photocatalytic activity for NO decomposition. *Res. Chem. Intermed.* 15(3):225-237.
- Anpo, M., Y. Ichihashi, and H. Yamashita. 1997. Developments of active titanium oxide catalyst for removal of NO_x and visible sensitive second generation titanium oxide photocatalyst. *Petrotech* 20(1):66-72.
- Atkinson, R. and S.M. Schmann. 1989. Rate constants for the gas-phase reactions of the OH radical with a series of aromatic-hydrocarbons at 296 +/- 2°K. *Int. J. Chem. Kinetics* 21(5):355-365.

- Ayoub, P.M. 1986. A transport reactor for photocatalytic reactions. Thesis. Northwestern University. Illinois.
- Bahnemann, D., D. Boeckelmann, and R. Goslich. 1991. Mechanistic studies of water detoxification in illuminated TiO₂ suspensions. *Sol. Energy Mater.* 24(1-4):564-583.
- Bickley, R.I., G. Munuera, and F.S. Stone. 1973. Photoadsorption and photocatalysis at rutile surfaces. II Photocatalytic oxidation of isopropanol. *J. Catal.* 31:398-407.
- Blake, D.M. 1999. Bibliography of work on the heterogeneous photocatalytic removal of hazardous compounds from water and air; Update Number 3 to January 1999. Golden, CO. National Renewable Energy Laboratory. NREL/TP-570-26797.
- Blake, D.M., J. Webber, C. Turchi, and K. Magrine. 1991. *Sol. Energy Mater.* 24:584
- Blake, N.R. and G.L. Griffin. 1988. Selectivity control during the photo-assisted oxidation of 1-butanol on titanium dioxide. *J. Phys. Chem.* 92:5697-5701.
- Blanco, J., P. Avila, A. Bahamonde, E. Alvarez, B. Sanchez, and M. Romero. 1996. Photocatalytic destruction of toluene and xylene at gas phase on a titania based monolithic catalyst. *Catal. Today* 29(1-4):437-442.
- Brinkley, D. and T. Engel. 1998a. Active site density and reactivity for the photocatalytic dehydrogenation of 2-propanol on TiO₂ (110). *Surf. Sci.* 415(3):L1001-L1006.
- Brinkley, D. and T. Engel. 1998b. Photocatalytic dehydrogenation of 2-propanol on TiO₂(110). *J. Phys. Chem. B* 102(39):7596-7605.
- Buechler, K.J., R.D. Noble, C.A. Koval, and W.A. Jacoby. 1999. Investigation of the effects of controlled periodic illumination on the oxidation of gaseous trichloroethylene using a thin film of TiO₂. *Indust. Engr. Chem. Res.* 38(3):892-896.
- Canela, M.C., R.M. Alberici, and W.F. Jardim. 1998. Gas-phase destruction of H₂S using TiO₂/UV-VIS. *J. Photochem. Photobiol. A: Chem.* 112(1):73-80.
- Cant, N.W. and J.R. Cole. 1992. Photocatalysis of the reaction between ammonia and nitric oxide on TiO₂ surfaces. *J. Catal.* 134:317-322.
- Cao, L.X., F.J. Spiess, A.M. Huang, S.L. Suib, T.N. Obee, S.O. Hay, and J.D. Freihaut. 1999. Heterogeneous photocatalytic oxidation of 1-butene on SnO₂ and TiO₂ films. *J. Phys. Chem. B* 103(15):2912-2917.
- Casado, J., J.M. Herrmann, and P. Pichat. 1990. Phototransformation of *o*-xylene over atmospheric solid aerosols in the presence of molecular oxygen and water. *Phys.- Chem. Behav. Atmos. Pollut. [Proc. Eur. Symp.]* 5:283-288.
- Courbon, H., J.M. Herrmann, and P. Pichat. 1981. Photocatalytic isotopic exchange between cyclopentane and deuterium over a bifunctional platinum/titanium dioxide catalyst. *J. Catal.* 72(1):129-138.

- Courbon, H., J.M. Herrmann, and P. Pichat. 1984. Effect of platinum deposits on oxygen adsorption and oxygen isotope exchange over variously pretreated, ultraviolet-illuminated powder titanium dioxide. *J. Phys. Chem.* 88(22):5210-5214.
- Courbon, H., J.M. Herrmann, and P. Pichat. 1985. Metal content and temperature effects on the photocatalytic isotopic exchange between cyclopentane and deuterium over Pt on Ni/TiO₂ in the normal SMSI state. *J. Catal.* 95:539.
- Courbon, H., M. Formenti, F. Juillet, A.A. Lisachenko, J. Martin, and S.J. Teichner. 1973. Photocatalytic activity of nonporous titanium dioxide (anatase). *Kinet. Catal.* 14:110-117.
- Cunningham, J. and B.K. Hodnett. 1981. Kinetic studies of secondary alcohol photo-oxidation on ZnO and TiO₂ at 348 K studied by gas chromatographic analysis. *J. Chem. Soc., Faraday Trans. 1* 77:2777-2801.
- Cunningham, J., E. Finn, and N. Samman. 1974. *Faraday Discuss. Chem. Soc.* 58:160.
- d'Hennezel, O. 1998. Chlorine-enhanced gas-solid photocatalysis : trichloroethylene promotion, TiO₂ pre-chlorination, mechanistic correlations, intermediates identification. Ph.D. thesis. North Carolina State and Ecole Centrale de Lyon.
- d'Hennezel, O. and D.F. Ollis. 1996. *Studies in Surf. Sci. Catal. 101, Part A*. J.W. Hightower, W.N. Delgass, E. Iglesia, and A.T. Bell, editors. Elsevier, Amsterdam. 435.
- d'Hennezel, O. and D.F. Ollis. 1997. Trichloroethylene - promoted photocatalytic oxidation of air contaminants *J. Catal.* 167:118.
- d'Hennezel, O., P. Pichat, and D.F. Ollis. 1998. Benzene and toluene gas-phase photocatalytic degradation over H₂O and HCL pretreated TiO₂: by-products and mechanisms. *J. Photochem. Photobiol. A - Chem.* 118(3):197-204.
- Dibble, L.A. and G.B. Raupp. 1990. Kinetics of gas-solid heterogeneous photocatalytic oxidation of trichloroethylene by near UV illuminated titanium dioxide. *Catal. Lett.* 4(4-6):345-354.
- Dibble, L.A. and G.B. Raupp. 1992. Fluidized-bed oxidation of trichloroethylene in contaminated air-streams. *Environ. Sci. Technol.* 26(3):492-495.
- Dreyer, M., G.K. Newman, L. Lobban, S.J. Kersey, R. Wang, and J.H. Harwell. 1997. Enhanced oxidation of air contaminants on an ultra-low density UV-accessible aerogel photocatalyst. *Mater. Res. Soc. Symp. Proc.* 454, Advanced Catalytic Materials-1996:141-146.
- Driessen, M.D. and V.H. Grassian. 1998. Photooxidation of trichloroethylene on Pt/TiO₂. *J. Phys. Chem. B* 102(8):1418-1423.
- Driessen, M.D., A.L. Goodman, T.M. Miller, G.A. Zaharias, and V.H. Grassian. 1998a. Gas-phase photooxidation of trichloroethylene on TiO₂ and ZnO: Influence of trichloroethylene pressure, oxygen pressure, and the photocatalyst surface on the product distribution. *J. Phys. Chem. B* 102(3):549-556.

- Driessen, M.D., T.M. Miller, and V.H. Grassian. 1998b. Photocatalytic oxidation of trichloroethylene on zinc oxide: characterization of surface-bound and gas-phase products and intermediates with FT-IR spectroscopy. *J. Molecular Catal. A - Chem.* 131(1-3):149-156.
- Edwards, M.E. 1994. Kinetics and intraparticle mass transfer limitations in photocatalytic systems. PhD Thesis. University of Wisconsin – Madison, pp. 114-116.
- Einaga, H., S. Futamura, and T. Ibusuki. 1999. Photocatalytic decomposition of benzene over TiO₂ in a humidified airstream. *Phys. Chem. Chemical Physics* 1(20):4903-4908.
- Formenti, M., F. Juillet, P. Meriaudeau, and S.J. Teichner. 1971. Heterogeneous photocatalysis for partial oxidation of paraffins. *Chem. Technol.* 1:680-686.
- Fox, M.A. 1983. Organic heterogeneous photocatalysis: chemical conversions sensitized by irradiated semi-conductors. *Acc. Chem. Res.* 16:314-321.
- Fox, M.A. 1991. Selective formation of organic compounds by photoelectrosynthesis. *Top. Curr. Chem.* 142:72.
- Fox, M.A., R.B. Draper, M.T. Dulay, and K. O'Shea. 1991. *Photochemical conversion and storage of solar energy*. E. Pelizzetti and N. Serpone, editors. Kluwer Academic Publishers, Dordrecht. 323.
- Fox, M.A. and M.T. Dulay. 1993. Heterogeneous photocatalysis. *Chem. Rev.* 93(1):341-357.
- Fu, X., L.A. Clark, W.A. Zeltner, and M.A. Anderson. 1996a. Effects of reaction temperature and water vapor content on the heterogeneous photocatalytic oxidation of ethylene. *J. Photochem. Photobiol. A - Chem.* 97(3):181-186.
- Fu, X., W.A. Zeltner, and M.A. Anderson. 1996b. Applications in photocatalytic purification of air. In *Semiconductor Nanoclusters*. P.V. Kamat and D. Meisel, editors. Elsevier Science B.V., 445-461.
- Fu, X., L.A. Clark, Q. Yang, and M.A. Anderson. 1996c. Enhanced photocatalytic performance of titania-based binary metal oxides: TiO₂/SiO₂ and TiO₂/ZrO₂. *Environ. Sci. Technol.* 30(2):647-653.
- Fu, X., W.A. Zeltner, and M.A. Anderson. 1995. The gas-phase photocatalytic mineralization of benzene on porous titania-based catalysts. *Appl. Catal. B-Environ.* 6(3):209-224.
- Fujishima, A. and K. Honda. 1972. Electrochemical photolysis of water at a semiconductor electrode. *Nature* 238:37-38.
- Fukumori, I. 1998. Tendency of development of photocatalytic coatings for air purification. *Toso to Toryo* 575:31-36.
- Gravelle, P.C., F. Juillet, P. Meriaudeau, and S.J. Teichner. 1971. Surface reactivity of reduced titanium dioxide. *Faraday Discuss. Chem. Soc.* 52:140.
- Herrmann, J.M., J. Disdier, and P. Pichat. 1981. Oxygen species ionosorbed on powder photocatalyst oxides from room-temperature photoconductivity as a function of oxygen pressure. *J. Chem. Soc., Faraday Trans. 1* 77(11):2815-2826.

- Hill, C.G., Jr. 1977. An introduction to chemical engineering kinetics and reactor design. John Wiley, New York.
- Hoffmann, M.R., S.T. Martin, W. Choi, and D.W. Bahnemann. 1995. Environmental applications of semiconductor photocatalysis. *Chem. Rev.* 95(1):69-96.
- Hoshi, K., H. Nameki, and T. Yamazaki. 1998. Developments of ceramics for removing pollutants from environment (Part VI) - Development of sound-absorbing ceramics with TiO₂ photocatalyst by recycling fused sewage slag and NO_x removal system. *Aichi-Ken Tokoname Yogyo Gijutsu Senta Hokoku* 25:1-6.
- Hung, C.H. and B.J. Mariñas. 1997a. Role of chlorine and oxygen in the photocatalytic degradation of trichloroethylene vapor on TiO₂ films. *Environ. Sci. Technol.* 31(2):562-568.
- Hung, C.H. and B.J. Mariñas. 1997b. Role of water in the photocatalytic degradation of trichloroethylene vapor on TiO₂ films. *Environ. Sci. Technol.* 31(5):1440-1445.
- Hung, C.H. and C.S. Yuan. 1998. Gas-phase photocatalytic degradation of perchloroethylene on glass pellets immobilized with TiO₂. *Proceedings of the Air & Waste Management Association 91st Annual Meeting & Exhibition*, June 14-18, San Diego, CA.
- Hwang, S.J., C. Petucci, and D. Raftery. 1998. *In situ* solid-state NMR studies of trichloroethylene photocatalysis: Formation and characterization of surface-bound intermediates. *J. Amer. Chem. Soc.* 120(18):4388-4397.
- Ibrahim, H. and H. de Lasa. 1999. Novel photocatalytic reactor for the destruction of airborne pollutants reaction kinetics and quantum yields. *Industr. Engr. Chem. Res.* 38(9):3211-3217.
- Ibusuki, T. and K. Takeuchi. 1986. Toluene oxidation on UV-irradiated titanium dioxide with and without O₂, NO₂ and H₂O at ambient temperature. *Atmos. Environ.* 20:1711-1715.
- Ichihashi, Y., H. Yamashita, and M. Anpo. 1997. Relationship between the local structures of titanium oxide photocatalysts and their reactivities - XAFS, UV, photoluminescence and photoreaction investigations. *J. De Physique Iv* 7(C2):883-885.
- Ishihara, S. and T. Furutsuka. 1996. Removal of NO_x or its conversion into harmless gases by charcoals and composites of metal oxides. *Prepr. Pap.- Am. Chem. Soc., Div. Fuel Chem.* 41(1):289-292.
- Isidorov, V., E. Klokova, V. Povarov, and S. Kolkova. 1997. Photocatalysis on atmospheric aerosols: Experimental studies and modeling. *Catal. Today* 39(3):233-242.
- Jacoby, W.A., D.M. Blake, J.A. Fennell, J.E. Boulter, L.M. Vargo, M.C. George, and S.K. Dolberg. 1996. Heterogeneous photocatalysis for control of volatile organic compounds in indoor air. *J. Air & Waste Manage. Assoc.* 46(9):891-898.
- Jacoby, W.A., Nimlos, M.R., Blake, D.M., Noble, R.D., and C.A. Koval. 1994. Products, intermediates, mass balances, and reaction pathways for the oxidation of trichloroethylene in air via heterogeneous photocatalysis. *Environ. Sci. Technol.* 28(9):1661-1668.
- Kaneco, S., H. Kurimoto, Y. Shimizu, K. Ohta, and T. Mizuno. 1999. Photocatalytic reduction of CO₂ using TiO₂ powders in supercritical fluid CO₂. *Energy* 24(1):21-30.

- Kennedy, J.C. and A.K. Datye. 1998. Photothermal heterogeneous oxidation of ethanol over Pt/TiO₂. *J. Catal.* 179(2):375-389.
- Kim, J.S., K. Itoh, and M. Murabayashi. 1996. Photocatalytic degradation of trichloroethylene on TiO₂ sol-gel thin films in gas phase: Effects of humidity on reaction rates, and analyses of products. *Yokohama Kokuritsu Daigaku Kankyo Kagaku Kenkyu Senta Kiyo* 22(1):17-21.
- Kim, J.S., K. Itoh, and M. Murabayashi. 1998. Photocatalytic degradation of trichloroethylene in the gas phase over TiO₂ sol-gel films: Analysis of products. *Chemosphere* 36(3):483-495.
- Kominami, H., J. Kato, S. Murakami, M. Kohno, Y. Kera, S. Nishimoto, M Inoue, T. Inui, and B. Ohtani. 2000. Thermal treatment of titanium alkoxides in organic media: novel synthesis methods for titanium (IV) oxide photocatalyst of ultra-high activity. *Stud. Surf. Sci. Catal.* 130B:1937-1942.
- Kudo, A. and H. Nagayoshi. 1998. Photocatalytic reduction of N₂O on metal-supported TiO₂ powder at room temperature in the presence of H₂O and CH₃OH vapor. *Catal. Lett.* 52(1-2):109-111.
- Larson, S.A. and J.L. Falconer. 1997. Initial reaction steps in photocatalytic oxidation of aromatics. *Catal. Lett.* 44(1-2):57-65.
- Larson, S.A., J.A. Widegren, and J.L. Falconer. 1995. Transient studies of 2-propanol photocatalytic oxidation on titania. *J. Catal.* 157(2):611-625.
- Li, K., S.Y.C. Liu, S. Khetarpal, and D.H. Chen. 1998. TiO₂ photocatalytic oxidation of toluene and PCE vapor in air. *J. Adv. Oxid. Technol.* 3(3):311-314.
- Lichtin, N.N., M. Avudaithai, and E. Berman. 1996. TiO₂-photocatalyzed oxidative degradation of binary mixtures of vaporized organic compounds. *Solar Energy* 56:377-385.
- Linsebigler, A., G. Lu, and J.T.Jr. Yates. 1995. Photocatalysis on TiO₂ surfaces: Principles, mechanisms, and selected results. *Chem. Rev.* 95(3):735-758.
- Linsebigler, A., C. Rusu, and J.T.Jr. Yates. 1996a. Absence of platinum enhancement of a photoreaction on TiO₂-CO photooxidation on Pt/TiO₂(110). *J. Am. Chem. Soc.* 118(22):5284-5289.
- Linsebigler, A., G. Lu, and J.T.Jr. Yates. 1996b. CO photooxidation on TiO₂ (110). *J. Phys. Chem.* 100(16):6631-6636.
- Liu, H., S.A. Cheng, J.Q. Zhang, C.N. Cao, and W.C. Jiang. 1997. The gas-photocatalytic degradation of trichloroethylene without water. *Chemosphere* 35(12):2881-2889.
- Liu, Y.C., G.L. Griffin, S.S. Chan, and I.E. Wachs. 1985. Photo-oxidation of methanol using MoO₃/TiO₂: catalyst structure and reaction selectivity. *J. Catal.* 94(1):108-119.
- Luo, Y. and D.F. Ollis. 1996. Heterogeneous photocatalytic oxidation of trichloroethylene and toluene mixtures in air: Kinetic promotion and inhibition, time-dependent catalyst activity. *J. Catal.* 163(1):1-11.
- Marinangeli, R.E. and D.F. Ollis. 1977. Photo-assisted heterogeneous catalysis with optical fibers. I Isolated single fiber. *AIChE* 23(4):415-426.

- Marinangeli, R.E. and D.F. Ollis. 1980. Photo-assisted heterogeneous catalysis with optical fibers. II Nonisothermal single fiber and fiber bundle. *AIChE* 26(6):1000-1006.
- Marinangeli, R.E. and D.F. Ollis. 1982. Photo-assisted heterogeneous catalysis with optical fibers. III Photoelectrodes. *AIChE* 28:946.
- Matsubara, H., M. Takada, S. Koyama, K. Hashimoto, and A. Fujishima. 1995. Photoactive TiO₂ containing paper: preparation and its photocatalytic activity under weak UV light illumination. *Chem. Lett.* 1995(9):767-768.
- Matthews, R.W. 1982. Solar-electric water purification using photocatalytic oxidation with TiO₂ as a stationary phase. *Solar Energy*. 38:405.
- Matthews, R.W. 1987. Photooxidation of organic impurities in water using thin films of titanium dioxide. *J. Phys. Chem.* 91(12):3328-3333.
- Méndez-Román, R. and N. Cardona-Martínez. 1998. Relationship between the formation of surface species and catalyst deactivation during the gas-phase photocatalytic oxidation of toluene. *Catal. Today* 40(4):353-365.
- Mills, A. and S. Morris. 1993. Photomineralization of 4-chlorophenol sensitized by titanium dioxide: A study of the initial kinetics of carbon dioxide photogeneration. *J. Photochem. Photobiol. A: Chem.* 71(1):75-83.
- Mozzanega, H., J.M. Herrmann, and P. Pichat. 1979. NH₃ oxidation over UV-irradiated TiO₂ at room temperature. *J Phys. Chem.* 83(17):2251-2255.
- Muggli, D.S. and J.L. Falconer. 1999. Parallel pathways for photocatalytic decomposition of acetic acid on TiO₂. *J. Catal.* 187(1):230-237.
- Muggli, D.S., K.H. Lowery, and J.L. Falconer. 1998. Identification of adsorbed species during steady-state photocatalytic oxidation of ethanol on TiO₂. *J. Catal.* 180(2):111-122.
- Muggli, D.S., S.A. Larson, and J.L. Falconer. 1996. Photocatalytic oxidation of ethanol: Isotopic labeling and transient reaction. *J. Phys. Chem.* 100(39):15886-15889.
- Mune, T., M. Sato, H. Kawahara, T. Ando, S. Ohhara, Y. Tanigami, and S. Cho. 1996. Deodorants miscible with organic substances. *Kogyo Zairyo* 44(8):114-118.
- Muradov, N.Z., A. Traissi, D. Muzzey, C.R. Painter, and M.R. Kemme. 1996. Selective photocatalytic destruction of airborne VOCs. *Solar Energy* 56(5):445-453.
- Murakami, H. and T. Ishida. 1996. Titanium oxide deodorizer filter. *Kogyo Zairyo* 44(6):57-61.
- Murata, Y., K. Kamitani, H. Tawara, and K. Takeuchi. 1998. Air purifying pavement. Development of photocatalytic concrete blocks for removal of NO_x. *Shigen to Sozai* 114(5):381-386.
- Negishi, N., T. Iyoda, K. Hashimoto, and A. Fujishima. 1995. Preparation of transparent TiO₂ thin film photocatalyst and its photocatalytic activity. *Chem. Lett.* 1995(9):841-842.

- Nimlos, M.R., E.J. Wolfrum, M.L. Brewer, J.A. Fennell, and G. Bintner. 1996. Gas-phase heterogeneous photocatalytic oxidation of ethanol: Pathways and kinetic modeling. *Environ. Sci. Technol.* 30(10):3102-3110.
- Nimlos, M.R., W.A. Jacoby, D.M. Blake, and T.A. Milne. 1993. Direct mass spectrometric studies of the destruction of hazardous wastes. 2. Gas-phase photocatalytic oxidation of trichloroethylene over TiO₂: products and mechanisms. *Environ. Sci. Technol.* 27(4):732-740.
- Nishikata, S. 1997. Apparatus for the removal of low concentration nitrogen oxides. *Kogyo Zairyo* 45(10):86-88.
- Noguchi, T., A. Fujishima, P. Sawunyama, and K. Hashimoto. 1998. Photocatalytic degradation of gaseous formaldehyde using TiO₂ film. *Environ. Sci. Technol.* 32(23):3831-3833.
- Obee, T.N. 1996. Photooxidation of sub-parts-per-million toluene and formaldehyde levels on titania using a glass-plate reactor. *Environ. Sci. Technol.* 30(12):3578-3584.
- Obee, T.N. and R.T. Brown. 1995. TiO₂ photocatalysis for indoor air applications: Effects of humidity and trace contaminant levels on the oxidation rates of formaldehyde, toluene and 1,3-butadiene. *Environ. Sci. Technol.* 29(5):1223-1231.
- Obee, T.N. and S. Satyapal. 1998. Photocatalytic decomposition of DMMP on titania. *J. Photochem. Photobiol. A - Chem.* 118(1):45-51.
- Obee, T.N. and S.O. Hay. 1997. Effects of moisture and temperature on the photooxidation of ethylene on titania. *Environ. Sci. Technol.* 31(7):2034-2038.
- Obee, T.N. and S.O. Hay. 1999. The estimation of photocatalytic rate constants based on molecular structure: Extending to multi-component systems. *J. Adv. Oxid. Technol.* 4(2):147-152.
- Obuchi, E., T. Sakamoto, K. Nakano, and F. Shiraiishi. 1999. Photocatalytic decomposition of acetaldehyde over TiO₂/SiO₂ catalyst. *Chem. Engr. Sci.* 54(10):1525-1530.
- Ohko, Y., A. Fujishima, and K. Hashimoto. 1998a. Kinetic analysis of the photocatalytic degradation of gas-phase 2-propanol under mass transport-limited conditions with a TiO₂ film photocatalyst. *J. Phys. Chem. B* 102(10):1724-1729.
- Ohko, Y., D.A. Tryk, K. Hashimoto, and A. Fujishima. 1998b. Autooxidation of acetaldehyde initiated by TiO₂ photocatalysis under weak UV illumination. *J. Phys. Chem. B* 102(15):2699-2704.
- Ohko, Y., K. Hashimoto, and A. Fujishima. 1997. Kinetics of photocatalytic reactions under extremely low-intensity UV illumination on titanium dioxide thin films. *J. Phys. Chem. A* 101(43):8057-8062.
- Ohno, T., T. Kigoshi, K. Nakabeya, and M. Matsumura. 1998. Stereospecific epoxidation of 2-hexene with molecular oxygen on photoirradiated titanium dioxide powder. *Chem. Lett.* 1998(9):877-878.
- Ohtani, B., S.W. Zhang, S. Nishimoto, and T. Kagiya. 1992. Catalytic and photocatalytic decomposition of ozone at room temperature over titanium(IV) oxide. *J. Chem. Soc. Faraday Trans.* 88(7):1049-1053.

- Ohtani, B., S.W. Zhang, T. Ogita, S. Nishimoto, and T. Kagiya. 1993. Photoactivation of silver loaded on titanium(IV) oxide for room-temperature decomposition of ozone. *J. Photochem. Photobiol. A: Chem.* 71:195-198.
- Okabe, K., K. Sayama, H. Kusama, and H. Arakawa. 1997. Photo-oxidative coupling of methane over TiO₂-based catalysts. *Chem. Lett.* 5:457-458.
- Ollis, D.F. 1985. Contaminant degradation in water - heterogeneous photocatalysis degrades halogenated hydrocarbon contaminants. *Environ. Sci. Technol.* 19:480-484.
- Ollis, D.F., E. Pelizzetti, and N. Serpone. 1991. Photocatalyzed destruction of water contaminants. *Environ. Sci. Technol.* 25:1523-1529.
- Peral, J. and D.F. Ollis. 1992. Heterogeneous photocatalytic oxidation of gas-phase organics for air purification: acetone, 1-butanol, butyraldehyde, formaldehyde and *m*-xylene oxidation. *J. Catal.* 136(2):554-565.
- Peral, J. and D.F. Ollis. 1997. TiO₂ photocatalyst deactivation by gas-phase oxidation of heteroatom organics. *J. Molecular Catal. A - Chem.* 115(2):347-354.
- Peral, J., X. Domenech, and D.F. Ollis. 1997. Heterogeneous photocatalysis for purification, decontamination and deodorization of air. *J. Chem. Tech. Biotech.* 70(2):117-140.
- Phillips, L.A. and G.B. Raupp. 1992. Infrared spectroscopic investigation of gas solid heterogeneous photocatalytic oxidation of trichloroethylene. *J. Molecular Catal.* 77(3):297-311.
- Pichat, P., J.M. Herrmann, J. Disdier, and M.N. Mozzanega. 1979. Photocatalytic oxidation of propene over various oxides at 320 K. Selectivity. *J. Phys. Chem.* 83(24):3122-3126.
- Plog, B. 1988. *Fundamentals of industrial hygiene*. National Safety Council, Chicago.
- Rao, N.N. and P. Natarajan. 1994. Particulate models in heterogeneous photocatalysis. *Current Sci.* 66(10):742-752.
- Raupp, G.B. and C.T. Junio. 1993. Photocatalytic oxidation of oxygenated air toxics. *Appl. Surf. Sci.* 72(4):321-327.
- Ren, P., Z. Tan, and W. Luo. 1995. Studies of thin layer photoelectric crystal. *Gongneng Cailiao* 26(2):138-140.
- Renz, C. 1921. Photo-reactions of the oxides of titanium, cerium and earth-acids. *Helv. Chim. Acta* 4:961.
- Sabate, J., M.A. Anderson, H. Kikkawa, M. Edwards, and C.G. Jr. Hill. 1991. A kinetic study of the photocatalytic degradation of 3-chlorosalicylic acid over TiO₂ membranes supported on glass. *J. Catal.* 127(1):167-177.
- Saitoh, T. and S. Fukayama. 1996. Photoactive TiO₂ thin films. *Zairyo Gijutsu* 14(5):133-137.
- Sampath, S., H. Uchida, and H. Yoneyama. 1994. Photocatalytic degradation of gaseous pyridine over zeolite-supported titanium-dioxide. *J. Catal.* 149(1):189-194.

- Sauer, M.L. and D.F. Ollis. 1994. Acetone oxidation in a photocatalytic monolith reactor. *J. Catal.* 149(1):81-91.
- Sauer, M.L. and D.F. Ollis. 1996. Photocatalyzed oxidation of ethanol and acetaldehyde in humidified air. *J. Catal.* 158(2):570-581.
- Sauer, M.L., M.A. Hale, and D.F. Ollis. 1995. *J. Photochem. Photobiol. A: Chem.* 88:169.
- Schiavello, M. 1988. *Photocatalysis and Environment*. Kluwer Academic, Dordrecht.
- Sclafani, A., L. Palmisano, M. Schiavello, and V. Augugliaro. 1988. *New J. Chem.* 12:129.
- Serpone, N. and E. Pelizzetti. 1989. *Photocatalysis: Fundamentals and Applications*. Wiley Interscience, New York.
- Seuwen, R. and P. Warneck. 1994. *Physico-Chemical Behavior of Atmospheric Pollutants* 1:137.
- Shifu, C., C. Xueli, T. Yaowu, and Z. Mengyue. 1998. Photocatalytic degradation of trace gaseous acetone and acetaldehyde using TiO₂ supported on fiberglass cloth. *J. Chem. Technol. Biotechnol.* 73:264-268.
- Sirisuk, A. 2003. Photocatalytic oxidation of ethylene over titanium dioxide supported on glass rings. PhD Thesis. University of Wisconsin – Madison, pp. 253-263.
- Sirisuk, A., C.G.Jr. Hill, and M.A. Anderson. 1999. Photocatalytic degradation of ethylene over thin films of titania supported on glass rings. *Catal. Today* 54(1):159-164.
- Sitkiewitz, S. and A. Heller. 1996. Photocatalytic oxidation of benzene and stearic acid on sol-gel derived TiO₂ thin films attached to glass. *New J. Chem.* 20(2):233-241.
- Sopyan, I., M. Watanabe, S. Murasawa, K. Hashimoto, and A. Fujishima. 1996a. An efficient TiO₂ thin-film photocatalyst: Photocatalytic properties in gas-phase acetaldehyde degradation. *J. Photochem. Photobiol. A - Chem.* 98(1-2):79-86.
- Sopyan, I., M. Watanabe, S. Murasawa, K. Hashimoto, and A. Fujishima. 1996b. Efficient TiO₂ powder and film photocatalysts with rutile crystal structure. *Chem. Lett.* 1996(1):69-70.
- Sopyan, I., S. Murasawa, K. Hashimoto, and A. Fujishima. 1994. Highly efficient TiO₂ film photocatalyst. Degradation of gaseous acetaldehyde. *Chem. Lett.* 1994(4):723-726.
- Sugawara, T. 1996. Application of photocatalysts for amenities. *Petrotech* 19(3):199-203.
- Suzuki, K., S. Satoh, and T. Yoshida. 1991. Photocatalytic deodorization on TiO₂ coated honeycomb ceramics. *Oenki Kagaku* 59:521-523.
- Takaoka, K. and I. Ebihara. 1995. Application of photocatalytic reaction to deodorizing sheets. *Kagaku Kogyo* 46(12):966-972.
- Takeda, N., M. Ohtani, T. Torimoto, S. Kuwabata, and H. Yoneyama. 1997. Evaluation of diffusibility of adsorbed propionaldehyde on titanium dioxide-loaded adsorbent photocatalyst films from its photodecomposition rate. *J. Phys. Chem. B* 101(14):2644-2649.

- Takeda, N., T. Torimoto, S. Sampath, S. Kuwabata, and H. Yoneyama. 1995. Effect of inert supports for titanium dioxide loading on enhancement of photodecomposition rate of gaseous propionaldehyde. *J. Phys. Chem.* 99(24):9986-9991.
- Takeuchi, K. 1995. Air-purifying sheets for cleaner streets. *Look Japan* December:24-25.
- Takeuchi, K. 1996. Air cleaning materials functioning by natural energy. *Kogyo Zairyo* 44(8):106-109.
- Takeuchi, K. and S. Kutsuna. 1996. Removal of chemical substances from the atmosphere by photocatalysis. *Shigen to Kankyo* 5(1):43-50.
- Toshiaki, F., T. Suzuki, and K. Sakamoto. 1997. Simultaneous removal of gases and particulates by photocatalyst and UV/photoelectron method. *Kuki Seijo* 35(3):169-176.
- Toshiaki, F., T. Suzuki, K. Sakamoto, S. Yokoyama, and M. Hirose. 1998a. Simultaneous removal of gaseous and particulate contaminants by a UV/photoelectron method - Super-cleaning of mini-environments. *Ebara Jiho* 180:3-14.
- Toshiaki, F., T. Suzuki, K. Sakamoto, S. Yokoyama, and M. Hirose. 1998b. Super cleaning of closed space by UV/photoelectron method using photocatalyst. *Earozoru Kenkyu* 13(2):110-118.
- Toth, Z., P. Penzeli, and E. Posan. 1995. Heterogeneous photocatalytic reduction of NO in the presence of conjugated polymers. *React. Kinet. Catal. Lett.* 56(1):185-190.
- Trivedik, D. 1994. Photocatalytic disinfection of airborne microorganisms. Thesis. University of Florida, Gainesville, Florida.
- Vergnon, P., J.M. Herrmann, and S.J. Teichner. 1978. Effect of particle sizes and doping on the catalytic activity of highly dispersed titanium dioxide. *Zh. Fiz. Khim.* 52(12):3021-3024.
- Vorontsov, A.V., E.N. Kurkin, and E.N. Savinov. 1999. Study of TiO₂ deactivation during gaseous acetone photocatalytic oxidation. *J. Catal.* 186(2):318-324.
- Vorontsov, A.V., E.N. Savinov, E.N. Kurkin, O.D. Torbova, and V.N. Parmon. 1997a. Kinetic features of the steady state photocatalytic CO oxidation by air on TiO₂. *React. Kinet. Catal. Lett.* 62(1):83-88.
- Vorontsov, A.V., E.N. Savinov, G.B. Barannik, V.N. Troitsky, and V.N. Parmon. 1997b. Quantitative studies on the heterogeneous gas-phase photooxidation of CO and simple VOCs by air over TiO₂. *Catal. Today* 39(3):207-218.
- Wallington, T.J., L.M. Skewes, and W.O. Siegl. 1988. *J. Photochem. Photobiol. A: Chem.* 45:167.
- Wang, K.H. and Y.H. Hsieh. 1998. Heterogeneous photocatalytic degradation of trichloroethylene in vapor phase by titanium dioxide. *Environ. Inter.* 24(3):267-274.
- Wang, K.H., H.H. Tsai, and Y.H. Hsieh. 1998a. A study of photocatalytic degradation of trichloroethylene in vapor phase on TiO₂ photocatalyst. *Chemosphere* 36(13):2763-2773.
- Wang, K.H., H.H. Tsai, and Y.H. Hsieh. 1998b. The kinetics of photocatalytic degradation of trichloroethylene in gas phase over TiO₂ supported on glass bead. *Appl. Catal. B-Environ.* 17(4):313-320.

- Wang, S., B. Raman, D.H. Chen, K.Y. Li, and J.A. Colapret. 1997. Photocatalytic oxidation of NO_x using TiO_2 and adsorbents. *Chem. Oxid.* 1995:5289-5302.
- Wentworth, W.E. and P.J. Chen. 1994. Photocatalytic reaction of 2-propanol over WO_3/SiO_2 using high-flux radiation. *Solar Energy* 52(3):253-263.
- Wolfrum, E.J., R. Rabago, and A.S. Jassal. 1997. *Destruction of volatile organic compound (VOC) emissions by photocatalytic oxidation (PCO): Final Report (ESHCOO3)*. Austin, TX. Sematech, Inc. 97013236A-ENG.
- Yamazaki, S., S. Tanaka, and H. Tsukamoto. 1999. Kinetic studies of oxidation of ethylene over a TiO_2 photocatalyst. *J. Photochem. Photobiol. A - Chem.* 121(1):55-61.
- Yamazaki-Nishida, S., K.J. Nagano, L.A. Phillips, S. Cervera-March, and M.A. Anderson. 1993. Photocatalytic degradation of trichloroethylene in the gas phase using titanium dioxide pellets. *J. Photochem. Photobiol. A: Chem.* 70(1):95-99.
- Yamazaki-Nishida, S., S. Cervera-March, K.J. Nagano, M.A. Anderson, and K. Hori. 1995. Experimental and theoretical study of the reaction mechanism of the photoassisted catalytic degradation of trichloroethylene in the gas phase. *J. Phys. Chem.* 99(43):15814-15821.
- Yamazaki-Nishida, S., X.Z. Fu, M.A. Anderson, and K. Hori. 1996. Chlorinated byproducts from the photoassisted catalytic oxidation of trichloroethylene and tetrachloroethylene in the gas phase using porous TiO_2 pellets. *J. Photochem. Photobiol. A: Chem.* 97(3):175-179.
- Yu, J.C., J. Lin, and W.M. Kwok. 1998. $\text{Ti}_{1-x}\text{Zr}_x\text{O}_2$ solid solutions for the photocatalytic degradation of acetone in air. *J. Phys. Chem. B* 102:5094-5098.
- Zorn, M.E., D.T. Tompkins, W.A. Zeltner, and M.A. Anderson. 1999. Photocatalytic oxidation of acetone vapor on $\text{TiO}_2/\text{ZrO}_2$ thin films. *Appl. Catal. B: Environ.* 23:1-8.
- Zorn, M.E., D.T. Tompkins, W.A. Zeltner, and M.A. Anderson. 2000. Catalytic and photocatalytic oxidation of ethylene on titania-based thin-films. *Environ. Sci. Technol.* 34:5206-5210.

TABLE TITLES

Table 1 Photocatalytic investigations: Some organic compounds of interest in indoor air applications.

Table 2 Some photocatalyst formulations.

Table 3 Light sources employed in photocatalytic reactors.

Table 4 Catalyst fouling and deactivation.

Table 5 Water vapor effect on a photocatalytic reaction.

Table 6 Kinetic models of PCO.

TABLES

Table 1

Gas	Primary Experimental Purpose	Reaction Products or Intermediates	Gas-Phase By-Products?*	Source
Ethanol (0, 100, 1000 ppm)	Identification and concentration of species on TiO ₂ surface as function of concentration of ethanol, O ₂ and water in feed	acetaldehyde, acetic acid, formaldehyde, formic acid	None detected	Muggli et al. (1998)
Toluene (13.1 ppm) (in 1342 ppm H ₂ O – 5% r.h.)	Identification of reaction intermediates	benzoic acid, benzaldehyde, benzyl alcohol, acetic acid, formic acid	None detected	d’Hennezel et al. (1998)
Benzene (15.5 ppm) (in 1342 ppm H ₂ O – 5% r.h.)	Identification of reaction intermediates	phenol, hydroquinone, 1,4-benzoquinone, acetic acid, formic acid	None detected	d’Hennezel et al. (1998)
Formaldehyde (30-2000 ppmv)	Investigate reaction characteristics	Formic acid during partial oxidation	None Detected	Noguchi et al. (1998)

*By-products other than CO₂ and H₂O in the gas-phase.

Table 2

Semiconductor Photocatalyst	Form (Powder / Thin-film / Particulate)	Supported?	Catalyst Source	Source
TiO ₂	Powder (anatase)	No (dispersed powder in liquid)	Wako Junyaku	Kaneco et al. (1999), Dibble & Raupp (1992)
TiO ₂	Thin-film (< 0.5 μm)	Yes (Pyrex)	Degussa P-25	Muggli et al. (1998)
1) TiO ₂ 2) TiO ₂ /H ₂ O 3) TiO ₂ /HCl	TiO ₂ powder (80% anatase)	Yes (Whatman glass microfiber filter)	Degussa P-25	d'Hennezel et al. (1998)
TiO ₂	Thin-film	Yes (inner wall of tube)	Sol-gel derived titania	Annapragada et al. (1997)
Cu ⁺ /SiO ₂ reduced Cu ²⁺ ions on SiO ₂	N/A	N/A	Ion-exchange method of preparation	Anpo et al. (1991)
TiO ₂	Titanium oxide catalyst and finely powdered TiO ₂ catalysts	Yes – anchored.	N/A	Anpo et al. (1995)
TiO ₂	Thin-film, 1.7 μm thick	Yes – to a soda lime glass flat surface	Sol-gel derived titania and Degussa P-25	Noguchi et al. (1998)

Table 3

Type	Nominal Power (W)	Irradiation	Manufacturer	Reference
Xe lamp	990	0.96 kW m ⁻²	Ushio Electronics Co.	Kaneco et al. (1999)
UV lamps	4	0.3 mW cm ⁻² ; 365 nm peak	GE	Muggli et al. (1998)
Hg lamp	125	Not measured; light pass through Corning 7-60 optical filter (300 nm < λ < 400 nm); 365 nm peak	Philips (HPK)	d'Hennezel et al. (1998)
UV lamps	4, 6, 8, 12, 40	variable, typically 2-10 mW cm ⁻² at and near surface of bulb.	WIKO (Japan) GTE Sylvania	Zorn et al. (2000), Wolfrum et al. (1997)
Hg-Xe	N/A	1 mW cm ⁻² at the surface of the thin-film photocatalyst	Hayashi Tokei, Luminar Ace 210	Noguchi et al. (1998)

Table 4

Gas	Effect of Gas on Catalyst	Regeneration Attempted? Approach	Source
Ethanol	Decreased rate of PCO due to accumulation of acetaldehyde on catalyst surface	N/A	Muggli et al. (1998)
Toluene, Benzene	Decreased rate of PCO possibly due to yellow viscous material settling between water and TiO ₂ ; products in material not identified but believed to be polymeric	Yes. Expose catalyst surface to airflow under UV radiation; regenerating for 16 hr was found effective; regenerating for 2-hr was ineffective; neither regenerating period allowed recovery of fresh TiO ₂ white color.	d'Hennezel et al. (1998)
Toluene	Catalyst deactivation	Yes. Activity was restored by illuminating the catalyst in the presence of hydrogen peroxide	Alberici and Jardim (1997)
<i>o</i> -xylene	Apparent loss in activity possibly due to low relative humidity, which favors the buildup of <i>o</i> -xylene and <i>o</i> -toluic acid on the catalyst surface	Yes. Pass humid air through the TiO ₂ reactor bed under continuous UV-irradiation	Ameen and Raupp (1999)

Table 5

Gas	Water Vapor	Source
Benzene (15.5 ppm)	Presence enhances PCO [H ₂ O] = 0, 1342, 10,800 ppmv	d'Hennezel et al. (1998)
<i>o</i> -xylene	Presence in low concentration increases the deactivation rate.	Ameen and Raupp (1999)
Trichloroethylene	PCO performance enhancement linked to reduction in the absolute water vapor concentration and competition between TCE and water vapor for adsorption sites on the catalyst.	Annapragada et al. (1997)
Formaldehyde, Toluene, and 1,3-butadiene	Humidity and contaminant concentrations on the oxidation rates are results of competitive adsorption	Obee and Brown (1995)
Ethylene	Water vapor concentration inversely related to rate of PCO	Fu et al. (1996a)

**Table 6a. Kinetic Models of PCO
Batch Reactor Operation**

Model	RXN Order	Rate Expression	Reactor Design Equation	Regression Plot (to determine <i>slope</i> and <i>intercept</i>)	Reaction Rate Constant, k_A Estimate	Units	Adsorp. Equil. Constant, K_A Estimate	Units
Power Law	1/2	$-r_A = k_A C_A^{1/2}$	$C_A^{1/2} = \frac{-k_A W}{2V_{res}} t + C_{A0}^{1/2}$	$C_A^{1/2}$ vs. t	$k_A = \frac{-2V_{res}}{W} \cdot slope$	$\text{mol}^{1/2} \cdot \text{l}^{1/2} \cdot \text{g}^{-1} \cdot \text{s}^{-1}$	-	-
	1 st	$-r_A = k_A C_A$	$\ln C_A = \frac{-k_A W}{V_{res}} t + \ln C_{A0}$	$\ln C_A$ vs. t	$k_A = \frac{-V_{res}}{W} \cdot slope$	$\text{l} \cdot \text{g}^{-1} \cdot \text{s}^{-1}$	-	-
	3/2	$-r_A = k_A C_A^{3/2}$	$C_A^{-1/2} = \frac{k_A W}{2V_{res}} t + C_{A0}^{-1/2}$	$C_A^{-1/2}$ vs. t	$k_A = \frac{2V_{res}}{W} \cdot slope$	$\text{l}^{3/2} \cdot \text{mol}^{-1/2} \cdot \text{g}^{-1} \cdot \text{s}^{-1}$	-	-
	2 nd	$-r_A = k_A C_A^2$	$C_A^{-1} = \frac{k_A W}{V_{res}} t + C_{A0}^{-1}$	C_A^{-1} vs. t	$k_A = \frac{V_{res}}{W} \cdot slope$	$\text{l}^2 \cdot \text{mol}^{-1} \cdot \text{g}^{-1} \cdot \text{s}^{-1}$	-	-
LH	-	$-r_A = \frac{k_A K_A C_A}{1 + K_A C_A}$	$\frac{\ln(1-f_A)}{f_A} = \frac{-k_A K_A W}{V_{res}} \frac{t}{f_A} + K_A C_{A0}$	$\frac{\ln(1-f_A)}{f_A}$ vs. $\frac{t}{f_A}$	$k_A = \frac{-V_{res} C_{A0}}{W \cdot intercept} \cdot slope$	$\text{mol} \cdot \text{g}^{-1} \cdot \text{s}^{-1}$	$K_A = intercept \cdot C_{A0}^{-1}$	$\text{l} \cdot \text{mol}^{-1}$

**Table 6b. Kinetic Models of PCO
Plug Flow Operation**

Model	RXN Order	Rate Expression	Reactor Design Equation	Regression Plot (to determine <i>slope</i> and <i>intercept</i>)	Reaction Rate Constant, k_A Estimate	Units	Adsorp. Equil. Constant, K_A Estimate	Units
Power Law	1/2	$-r_A = k_A C_A^{1/2} = k_A C_{A0}^{1/2} \sqrt{1-f_A}$	$\sqrt{1-f_A} = -\frac{k_A C_{A0}^{1/2}}{2} \cdot \frac{W}{F_{A0}} + 1$	$\sqrt{1-f_A}$ vs. W/F_{A0}	$k_A = \frac{-2 \cdot \text{slope}}{C_{A0}^{1/2}}$	$\text{mol}^{1/2} \cdot \text{l}^{1/2} \cdot \text{g}^{-1} \cdot \text{s}^{-1}$	-	-
	1 st	$-r_A = k_A C_A = k_A C_{A0} (1-f_A)$	$\ln(1-f_A) = -k_A C_{A0} \cdot \frac{W}{F_{A0}}$	$\ln(1-f_A)$ vs. W/F_{A0}	$k_A = \frac{-\text{slope}}{C_{A0}}$	$\text{l} \cdot \text{g}^{-1} \cdot \text{s}^{-1}$	-	-
	3/2	$-r_A = k_A C_A^{3/2} = k_A C_{A0}^{3/2} (1-f_A)^{3/2}$	$\frac{1}{\sqrt{1-f_A}} = \frac{k_A C_{A0}^{3/2}}{2} \cdot \frac{W}{F_{A0}} + 1$	$1/\sqrt{1-f_A}$ vs. W/F_{A0}	$k_A = \frac{2 \cdot \text{slope}}{C_{A0}^{3/2}}$	$\text{l}^{3/2} \cdot \text{mol}^{-1/2} \cdot \text{g}^{-1} \cdot \text{s}^{-1}$	-	-
	2 nd	$-r_A = k_A C_A^2 = k_A C_{A0}^2 (1-f_A)^2$	$\frac{1}{1-f_A} = k_A C_{A0}^2 \cdot \frac{W}{F_{A0}} + 1$	$1/(1-f_A)$ vs. W/F_{A0}	$k_A = \frac{\text{slope}}{C_{A0}^2}$	$\text{l}^2 \cdot \text{mol}^{-1} \cdot \text{g}^{-1} \cdot \text{s}^{-1}$	-	-
LH	-	$-r_A = k_A \theta_A = \frac{k_A K_A C_A}{1 + K_A C_A}$	$\frac{f_A}{\ln(1-f_A)} = k_A \frac{W}{F_{A0} \ln(1-f_A)} + \frac{1}{K_A C_{A0}}$	$\frac{f_A}{\ln(1-f_A)}$ vs. $\frac{W}{F_{A0} \cdot \ln(1-f_A)}$	$k_A = \text{slope}$	$\text{mol} \cdot \text{g}^{-1} \cdot \text{s}^{-1}$	$K_A = (\text{intercept} \cdot C_{A0})^{-1}$	$\text{l} \cdot \text{mol}^{-1}$

FIGURE CAPTIONS

Figure 1 Steps in photoelectrochemical mechanisms in solid semiconductor: [1] light energy $h\nu$ greater than band gap energy E_g [2] excites electron from valence band to conduction band; [3] valence-band hole that successfully migrates to surface initiates oxidative pathway; [4] conduction-band electron that successfully migrates to surface initiates reduction reaction; [5] valence-band hole and conduction-band electron recombine in the bulk material; [6] valence-band hole and conduction-band electron recombine on the surface; [7] trapping of valence-band hole at a surficial titanol group; [8] trapping of conduction-band electron in surficial bond. Adapted from Linsebigler et al. (1995) and Hoffman et al. (1995).

Figure 2 Diagram of powder layer photocatalytic reactor. Design employed by Teichner's group. Adapted from Formenti et al. (1971).

Figure 3 Annular reactor where d_o is lamp diameter, D_i is reactor inner wall diameter, and D_o is reactor outer wall diameter. Design adapted from Ayoub (1986) and Fu et al. (1995).

Figure 4 Fluidized bed PCO reactor. Design employed and adapted by Dibble and Raupp (1992).

Figure 5 Light irradiance of fluorescent bulbs (F8T5BL) labeled Y1 and Y2 during continual operation.

FIGURES

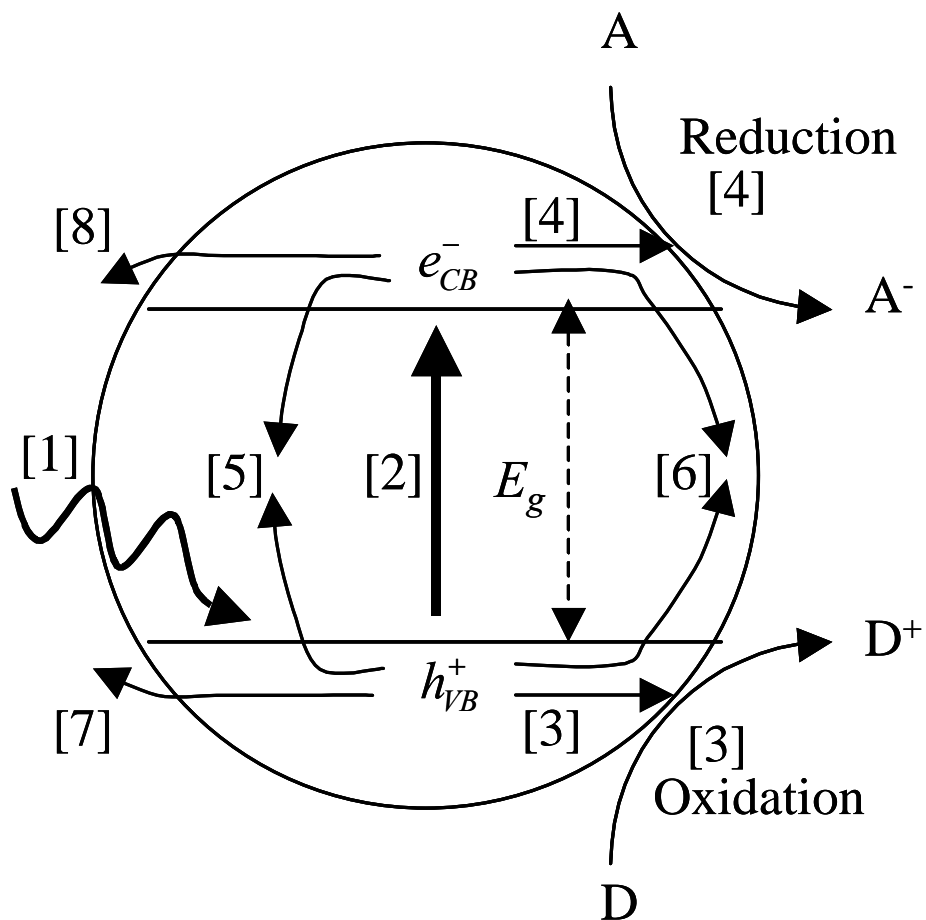


Figure 1

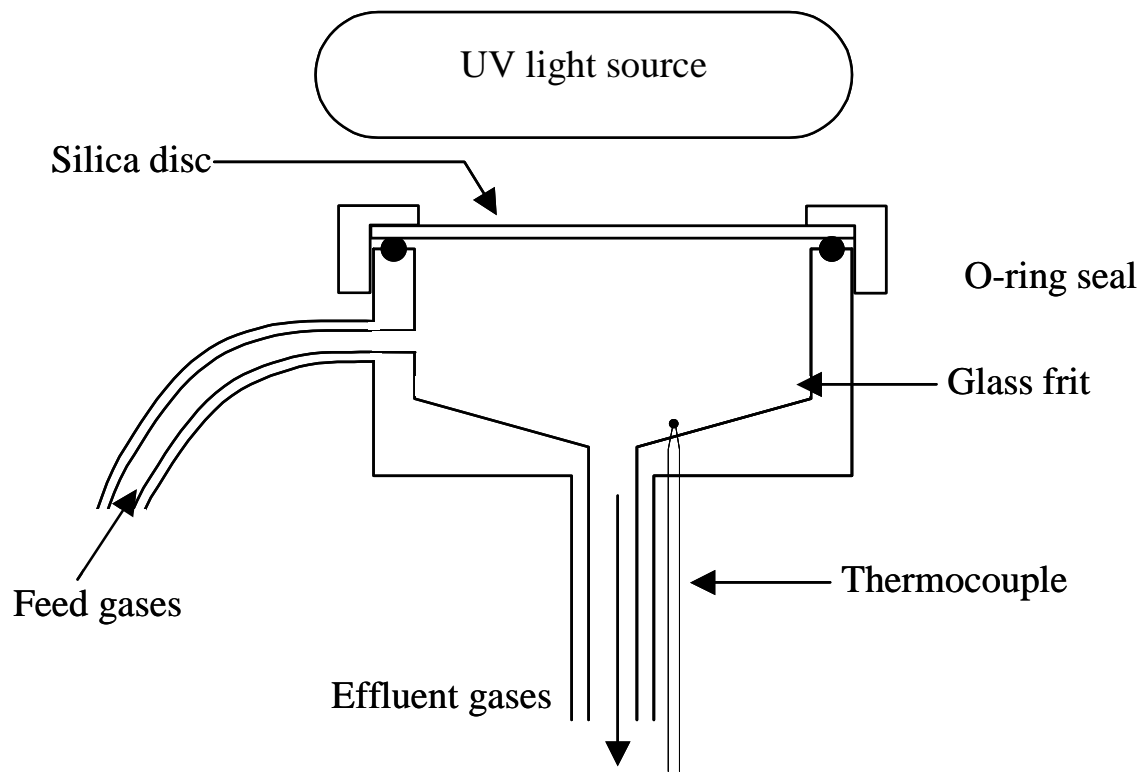
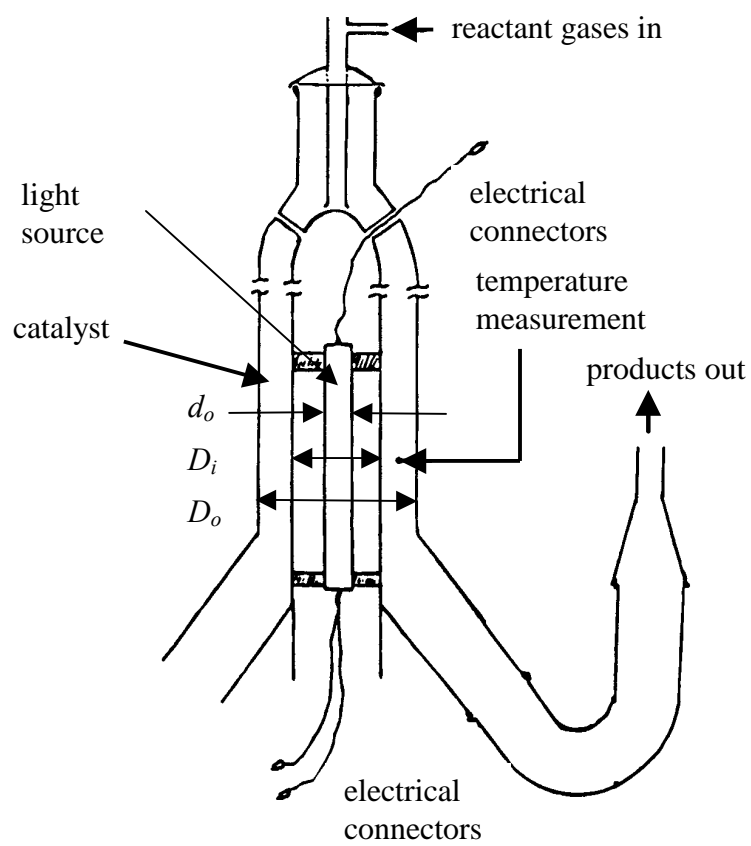


Figure 2

**Figure 3**

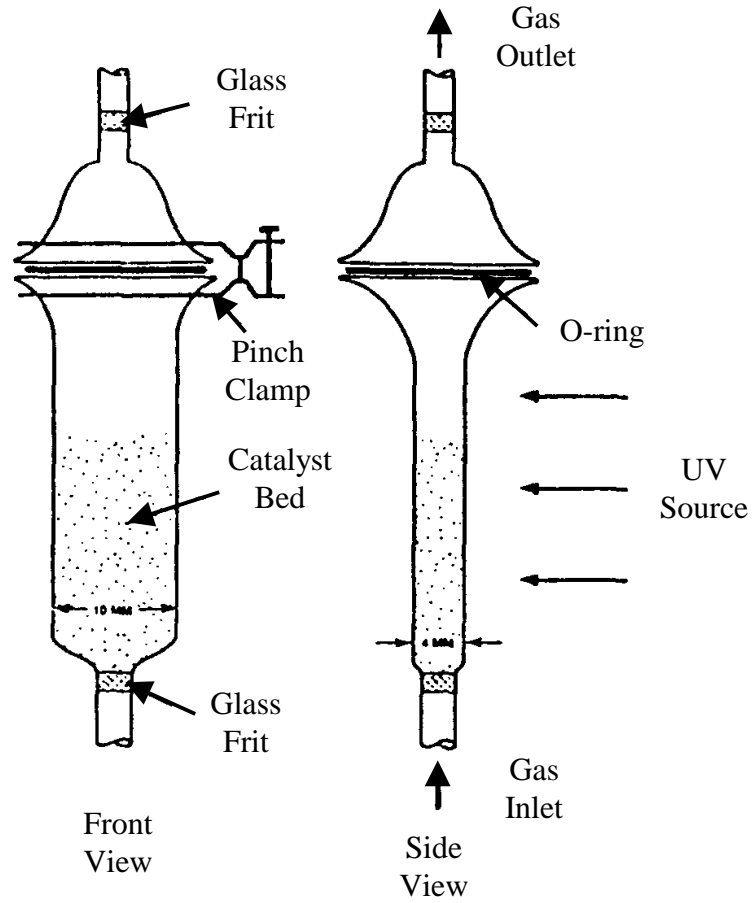


Figure 4

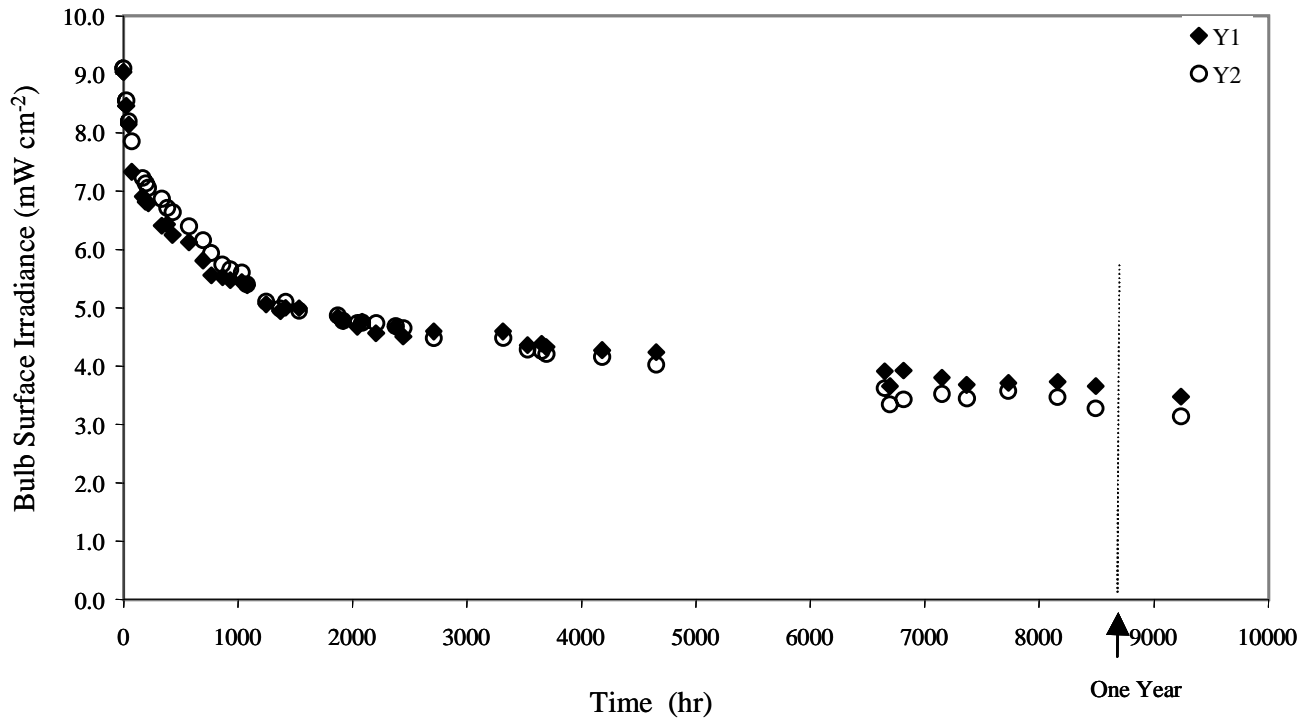


Figure 5

Evaluation of Photocatalysis for Gas-Phase Air Cleaning – Part 2: Economics and Utilization

Dean T. Tompkins, PhD, PE (ASHRAE Member)

Ben J. Lawnicki, BS

Walter A. Zeltner, PhD

Marc A. Anderson, PhD

ABSTRACT

Several approaches to estimate the cost of installing and operating a photocatalytic oxidation (PCO) device for application in various treatment concerns are presented. First, a simplified approach for estimating the cost of a PCO device using laboratory data is presented in some detail. Second, the cost of ownership of a PCO device for treating outgases from soils contaminated with liquid solvents is compared with other treatment technologies including granular activated carbon (GAC) and groundwater extraction with liquid phase UV/peroxidation. Third, a study based on a consortium of semi-conductor companies demonstrated that the cost of ownership of a PCO for point-of-use (POU) applications is not likely to cost less on a “per CFM basis” than existing end-of-pipe (EOP) technologies. However, the study findings indicated that in a number of specific cases PCO may provide a cost-effective alternative to EOP technologies. Last, a report was published comparing the first and operating costs of PCO vs. GAC. The study reported that (1) due to the high first and operating costs of PCO device compared with the GAC approach, PCO is not likely to replace GAC as a technology for treating a steady-state inlet feed of VOCs; and (2) PCO can improve in this comparison (to GAC) if improved catalysts capable of high reaction rates and quantum yields are developed and if lower cost low-pressure mercury-vapor lamps can be employed as a substitute for the medium-pressure lamps.

KEYWORDS: Air cleaning, air pollution control, catalysis, environmental control, filtration, gas, indoor air quality, photocatalysis

D.T. Tompkins is associate scientist, Water Science and Engineering Laboratory, University of Wisconsin – Madison, Madison, WI; B.J. Lawnicki is process engineer, Intel Massachusetts, Hudson, MA; W.A. Zeltner is associate scientist, Water Science and Engineering Laboratory, University of Wisconsin – Madison, Madison, WI; M.A. Anderson is professor, Department of Civil and Environmental Engineering, University of Wisconsin – Madison, Madison, WI.

INTRODUCTION

A significant challenge created, in part, by the Clean Air Act Amendments of 1990 (CAAA) is identifying efficient and economical technologies to control the concentrations of volatile organic compounds (VOCs). Several technologies have been identified as existing or emerging end-of-pipe VOC abatement and control technologies including – thermal oxidizers (thermal incinerators), catalytic oxidizers (catalytic incinerators), condensers, adsorbers, biofilters, membrane separators, corona destruction reactors, plasma reactors and ultraviolet (UV) oxidizers (Moretti and Mukhopadhyay 1993). Thermal and catalytic oxidizers, condensers, and adsorbers are popular VOC control technologies because of their broad applicability. Oxidizers combust VOCs, which are destroyed without recovery. Conversely, adsorbers and condensers are recovery devices, in which VOCs are recovered and can be occasionally reused. Biofiltration, membrane separation, and UV oxidation technologies represent the newest of these technologies.

UV catalytic or photocatalytic oxidation (PCO) is a technology that can treat low-level concentrations of gas contaminants found in indoor air. The oxidant used in PCO is the 20% of oxygen present in air. Because the concentration of oxygen in air is so much larger than the (total) concentration of gaseous indoor air pollutants, it is not necessary to employ additional oxidants such as ozone (O_3) or hydrogen peroxide (H_2O_2). In this paper, the economics and utilization of PCO as a technology to treat contaminants in feed streams of air is addressed.

MAIN BODY

Cost Analysis

This analysis is concerned with the costs associated with a photocatalytic oxidation system including the capital cost (or initial investment) and the (periodic) operating costs. An analysis is performed on a commercial-scale photocatalytic system for a specific application for the food industry. The analysis is salient for it discusses a mathematical model that can be used to size a PCO system for a specific application. Although used herein for a specific case, the model can be applied to other situations,

thereby broadening its applicability. In addition, other approaches to conduct engineering analyses are presented based on information presented in prior publications – both peer-reviewed journal form and conference proceedings.

The analyses reported herein are for photocatalytic systems that may be employed in large-scale applications including commercial buildings. However, most peer-reviewed, publicly available PCO data to date are based on laboratory bench-top experiments that typically entail low volumetric flow rates, one to a few reactant compounds, and small reactor sizes.. Therefore, estimates of the first cost of PCO systems for application in commercial buildings are often based on linearly scaling the cost of these smaller PCO systems.

Photocatalytic Reactor Sizing Approach & Cost Analysis

The methodology employed by the present investigators to size and cost a PCO reactor was adapted from cost models of other investigators (Turchi et al. 1995, Turchi et al. 1994). The methodology to size a photocatalytic reactor and prepare cost predictions for commercial-scale (prototype) photocatalytic reactors is depicted in Figure 1. This approach is initiated by identifying one (or a few) test gas(es) to be treated. After selecting a suitable reactor configuration (i.e., bulb-catalyst ratio and reactor configuration), one selects a particular catalyst type and reactor temperature to begin to generate laboratory data. If there are by-products formed in these studies, then one must consider adopting an alternative catalyst formulation or different reaction conditions. When no reaction by-products are produced, then several experiments can be performed to generate kinetic data. Upon achieving an acceptable fit of laboratory data with the kinetic model, it is possible to estimate the size of the PCO reactor and perform an analysis to determine the cost of ownership. If the cost of the unit is commercially acceptable, then production of a prototype can begin. If the cost is unacceptable, one must consider a different catalyst formulation, a different reactor configuration, a different set of operating conditions, or consider a different sequestering technology.

Sizing Approach & Cost Analysis - Based on a University-Corporate Collaborative Approach

The following is a systematic approach for predicting the cost of a commercial-scale PCO reactor for use in a building environment. The cost analysis is performed for a low flow-rate, commercial-scale PCO reactor that is based on a university-corporate collaborative project. An engineering cost analysis of a commercial-scale PCO reactor for a higher flow-rate application in building environments is based on the underlying assumptions and linear extrapolation of the costs for the lower flow-rate system.

Presently, it is accepted that the design of photocatalytic oxidation reactors (PORs) should be application driven, with each application focused on a basic set of relevant VOC species. This approach suggests that a model is required to tailor each application to the species involved. The approach is enumerated as follows:

- 1) A design equation (i.e., rate expression for kinetic modeling) for the POR is selected and suitably modified for usage.
- 2) A suitable number of experiments are performed with the relevant VOC(s).
- 3) The empirical data is fitted with the design equation to determine the reaction rate constant for the species.
- 4) The rate constant is employed in the (original) design equation to determine the amount of photocatalyst required for a given set of conditions including volume of air to be treated, and the initial and final concentrations of the VOC in the building.
- 5) A relationship between the amount of photocatalyst required for an application and the cost of the POR is employed to estimate the cost of the POR.
- 6) Operating costs are then determined based on power usage of the POR and annual maintenance needs.

Each step of this process is demonstrated here. The present analysis assumes that there is no generation of the contaminant within the enclosed space.

Step 1) Design Equation for POR

Assuming that the photocatalytic oxidation of a VOC follows a power law model, we have

$$r_A = k_A C^n = -\frac{V_{res}}{W} \frac{dC}{dt} \quad (1)$$

In Eq. 1, r_A is the reaction rate ($\text{mol g}^{-1} \text{s}^{-1}$), k_A is the reaction rate constant (units depend on n), C is the concentration of species A or the VOC-of-interest (mol L^{-1}) (i.e., the VOC that one desires to remove from an enclosure via oxidation), n is the order of the reaction with respect to the disappearance (or conversion) of the VOC, V_{res} is the volume of the *reservoir* (e.g., the volume of the room or building in which the VOC is present), W is the mass of the catalyst (g), and t is the time for the reaction (s). [Since the concentration of the VOC in an enclosure being treated with the POR decreases with time, the term dC/dt is negative, and a negative sign is required on the right-hand-side of Eq. 1.] The design equation model exemplified by Eq. 1 follows directly from first principles developed previously (Edwards 1994). Equation 1 has been used successfully to model the concentration of a VOC in a closed system when treated by a PCO device, where the reactor was operating as a *batch* reactor (Zorn et al. 2000). This type of model has implications in its ability to predict performance and will be discussed later.

A solution for Eq. 1 is found by separating variables and integrating

$$\frac{k_A W}{V_{res}} \int_{t=0}^{t=t} dt = - \int_{C_{A0}}^{C_A} \frac{dC}{C^n} = - \int_{C_{A0}}^{C_A} C^{-n} dC \quad (2)$$

In Eq. 2, C_{A0} is the initial concentration of the VOC-of-interest in an enclosure at time 0 and C_A is the concentration of the VOC at some later time t . Rearranging Eq. 2 will give

$$\int_{C_{A0}}^{C_A} C^{-n} dC = -\frac{k_A W}{V_{res}} t \quad (3)$$

Equation 3 is a general form of a reactor design equation. In order to integrate the left-hand-side of Equation 3, it is necessary to have a numerical value for n . A suitable value for n may be found in the literature for a given reactant species and set of reaction conditions. However, a standard approach to solving Eq. 3 is to estimate a value for n and then test that choice for n against concentration-vs.-time

data obtained from experiments. To elaborate on this approach and for edification, two choices for n will be evaluated and the results of both choices are presented below. (Note, while it will appear that both numerical selections for n are random, the authors have pre-selected two particular n 's. The choices are $n = 1/2$ and $n = 4/5$; Eq. 3 is evaluated as follows

$$n = 1/2 : \quad \int_{C_{A0}}^{C_A} C^{-1/2} dC = \frac{C^{1/2}}{1/2} \Big|_{C_{A0}}^{C_A} = C_A^{1/2} - C_{A0}^{1/2} = -\frac{k_A W}{2V_{res}} t \quad (4a)$$

$$C_A^{1/2} = C_{A0}^{1/2} - \frac{k_A W}{2V_{res}} t \quad (4b)$$

$$n = 4/5 : \quad \int_{C_{A0}}^{C_A} C^{-4/5} dC = \frac{C^{1/5}}{1/5} \Big|_{C_{A0}}^{C_A} = C_A^{1/5} - C_{A0}^{1/5} = -\frac{k_A W}{5V_{res}} t \quad (5a)$$

$$C_A^{1/5} = C_{A0}^{1/5} - \frac{k_A W}{5V_{res}} t \quad (5b)$$

Since Eq. 4b and 5b are in a linear form, the slope of the line fitting the data can be used to find the reaction rate constant (k_A). So, for

$$n = 1/2 : \quad k_A = -slope \frac{2 V_{res}}{W} \quad (6)$$

where k has units of $\text{mol}^{1/2} \text{L}^{1/2} \text{g}^{-1} \text{s}^{-1}$; and for

$$n = 4/5 : \quad k_A = -slope \frac{5 V_{res}}{W} \quad (7)$$

where k has units of $\text{mol}^{1/5} \text{L}^{4/5} \text{g}^{-1} \text{s}^{-1}$. (Note: The units of k depend on the selection of n .) The value for *slope* in Eq. 6 and 7 is the slope of the curve used to approximate the data obtained from conversion experiments.

Step 2) Conversion Experiments

At a minimum, one PCO experiment should be performed under a set of known conditions—a fixed reactor design (that is, a fixed light irradiance-to-catalyst ratio), temperature, %RH, and initial concentration of the VOC-of-interest. (It is recommended that experimental conditions most closely

match those of the application, in particular the initial concentration of the reactant.) An experiment to photocatalytically oxidize ethylene was performed in a gas-tight testing chamber (V_{res}) of 10,000 L with an initial concentration (C_{A0}) of 3.88×10^{-7} mol L⁻¹ (9.5 ppmv), a final VOC concentration (C_A) of 2.86×10^{-9} mol L⁻¹ (0.07 ppmv) which took 18.2 hours (t) with a reactor that has 3.58 g of catalyst (W). (NOTE: W is the mass of the catalyst, not the mass of the catalyst and its support.) The ethylene concentration data in the chamber at several times during the experiment are provided in Table 1. (Note: This experiment was performed recently by a business entity that markets photocatalytic equipment; in short, the data in Table 1 are from an actual experiment.)

Step 3) Data Approximation with Kinetic Model

Upon completing the experiment, the data can be plotted for the $n = 1/2$ model (Fig. 2) and $n = 4/5$ model (Fig. 3). As evident from the approximations, the 4/5-order model more accurately fits the data. Now, the *slope* in Fig. 3 and Eq. 7 are used to compute the reaction rate constant (k_A) as 6.99×10^{-3} mol^{1/5} L^{4/5} g⁻¹ s⁻¹.

Step 4) Determination of Catalyst Amount

Since n and k_A are known, one can employ Eq. 5b to estimate the mass of catalyst needed to treat an enclosure under a given set of reaction conditions. In other words, the rate constant and reaction order are employed to determine the mass (W) of photocatalyst required for a given set of conditions including volume of air to be treated (V_{res}), initial (C_{A0}) and desired final (C_A) concentrations of the VOC in the building, and the amount of time (t) required to treat the VOC contaminant in the building. This relationship (Eq. 5b) is plotted in Fig. 4 for conditions where 95% of the target specie (ethylene) was removed in 24 hours by passing the enclosure's air through a reactor. The amount of catalyst needed to oxidize ethylene with the photo-reactor for three initial concentrations ($C_{A0} = 1, 10,$ and 100 ppmv) in the enclosure is determined.

For the conditions displayed in Fig. 4, consider both a residential application (2,000 ft²) and a commercial building application (20,000 ft²), both with 8 ft ceilings, giving a treatment volume (V_{res})

of 4.528×10^5 and 4.528×10^6 L, respectively. The mass of catalyst needed to remove ethylene from the residence is 89 g and from the commercial building application 891 g for an initial ethylene concentration of 10 ppmv. Note that these estimates for the weight of the catalyst needed to treat a feed stream of ethylene are quite high because ethylene is difficult to photocatalytically oxidize because it is non-polar, symmetric, has a high vapor pressure (low boiling point), and is a small molecule that is not easily adsorbed onto photocatalytic surfaces. In other words, other VOCs-of-interest in indoor environments will readily produce higher reaction rate constants than that achieved with ethylene, thereby reducing the amount of catalyst (and size of the reactor) needed to treat a given indoor air application. For example, consider the amount of catalyst needed to photocatalytically oxidize a compound that can be modeled with a 4/5-reaction order and has a reaction rate constant that is two orders of magnitude larger than that obtained for ethylene (Fig. 5). Note that the analyses above assume that the reaction rate constant for ethylene oxidation is independent of the initial concentration. Such an assumption is not always upheld.

Step 5) Capital Cost Estimate of Photo-reactor

The cost of a photo-reactor to treat ethylene gas has been provided by the original equipment manufacturer (OEM), which is in commercial-scale production. The cost data and most details of the reactor design are proprietary to the manufacturer for treating a known volume (V_{res}) and an initial concentration (C_{A0}). Reactor information that can be shared includes the catalyst mass of 3.58 grams, supplemental heat required to maintain the reactor operating at 70°C, and continuous reactor operation. Therefore, for this application the cost data are real and have been implemented into cost estimates below. If it is assumed that the cost of a photo-reactor scales linearly with the volume of the enclosure to be treated, then the cost for a photo-reactor is found in Fig. 6 and 7, for ethylene and an *easier-to-oxidized* gas, respectively. The cost data in Fig. 6 and 7 reflect a retail mark-up (factor) of 3.1. Therefore, to obtain an OEM cost for the POR divide the cost in Fig. 6 and 7 by 3.1.

Step 6) Operating Cost of Photo-reactor

Operating costs of the photo-reactor are determined based on power usage and maintenance/replacement cost.

Power Cost. For the case of the commercial application of the photo-reactor described in Step 5, the current draw (power usage) is 7.1 amps (120 VAC) when supplemental heat is required and 3.1 amps when supplemental heat is not required. For the purpose of this study we will assume that supplemental heat is required continuously. Annual maintenance costs are based on need.

Maintenance/Replacement Cost. Based on data and discussions herein, it is recommended to replace the light sources annually and the catalyst biannually. For the case of the commercial application of the photo-reactor described in Step 5, replacement cost for the light sources and catalyst and labor to effect the replacement is estimated to be \$375.

Sizing Approach & Cost Analysis - Based on a Corporate Approach

A few commercial-scale photocatalytic systems are employed presently to treat outgases from soils contaminated with liquid solvents. While these applications are different than those that might employ a PCO unit in a building environment, a successful field demonstration of a commercial-scale installation has demonstrated that photocatalysis offers economic and operational advantages over competitive approaches (Brunet et al. 1999). For example, consider a remediation project that employed multi-phase extraction to achieve rapid remediation of a site. The photocatalytic technology produced flow rates of 700 scfm. In an economic analysis, the EPA's selection for a remedy for the site was soil vapor extraction followed by activated carbon treatment in combination with groundwater pumping and UV/peroxide oxidation. The estimated life of the soil vapor extraction was four years, and the groundwater pumping was estimated to have a thirty-year life cycle. An alternative remedy was proposed which combined emissions from soil vapor extraction and a ground water air stripper, treating the mixed VOCs using UV photocatalysis. An economic analysis of the two points was conducted to justify the approach, and the alternative – UV photocatalysis – was installed. The results of the economic comparison are presented in Tables 2 and 3.

The actual operating and capital cost data from the 1998 season were used for the installed option, and compared with the EPA estimates. Using an interest rate factor of 7%, a four-year life cycle for soil vapor extraction, and a thirty-year life cycle for groundwater pumping, a savings in Net Present Cost (NPC) of \$2,183,782 was determined for the option containing UV photocatalysis (Brunet et al. 1999). The operating costs account for tri-annual catalyst replacement, annual lamp replacement, electric power, caustic for acid neutralization, soil monitoring, and labor costs. Power costs for soil vapor extraction pumps are not included. Capital costs are for actual expenditures for all equipment on site, including the air stripper and caustic scrubber.

Sizing Approach & Cost Analysis - Based on a Consortium Approach

The consortium of semiconductor manufacturing companies, Sematech (Austin, TX), commissioned a study to evaluate the use of photocatalytic oxidation as a volatile organic compound control technology for point-of-use (POU) application in the semiconductor industry. The study is reported by Wolfrum et al. (1997) and contains the results of laboratory-scale testing and presents estimates of the cost of ownership (COO) of PCO for POU applications. Testing was conducted at a commercial company for two reasons: 1) to collect adequate experimental data to permit a commercial company to provide a cost estimate of a full-scale treatment system and (2) to investigate the performance of the commercial company's PCO system. The study reported several conclusions:

1. Assumptions in the design: The POR design basis employed for the cost analysis will treat 500 ppmv methanol at a flow rate of 1000 scfm. The conceptual POR design is a 75-lamp system (each lamp 48" long, drawing 62 W). The reactor is a cube measuring 4 feet on an edge. Supplemental heat is provided to achieve an operating temperature of 70°C. The cost of a reactor is estimated at about \$60,000. This cost is in agreement with both the literature correlation the National Renewable Energy Laboratory (NREL) has used in the past and an approximate calculation based on materials of construction and required construction labor hours. Table 4 contains the results of the Sematech COO analysis for the four treatment systems considered.
2. Based on experimental results, NREL and the commercial company independently developed estimates for the capital and operating costs of a PCO system operating at 1000 scfm. NREL then used the Sematech COO model to determine COO. The results suggest that a 1000 CFM PCO system would have a COO of approximately \$25,000-\$30,000 per 1000 CFM. The Sematech estimate for current end-of-pipe (EOP) thermal technologies is approximately \$20,000 per 1000 CFM.
3. Based on results of the COO model, the study concluded that it appears unlikely that photocatalytic oxidation will cost less on a "per CFM basis" than existing EOP technologies. However, a number of specific cases indicate that POU technologies in general and photocatalytic oxidation in particular may provide a cost-effective alternative to EOP technologies. The study also concluded that the actual costs of these specific cases are not well captured by the COO model.
4. For the design basis used, photocatalytic technology appears to be better than conventional (catalytic) technology for POU. Corporate entity #3 also produces an adsorption system, but recommends their catalytic oxidation system because the relatively high methanol inlet concentration (500 ppmv) in the stream would result in a concentrated methanol stream during regeneration of the adsorption-based technology that is very close to the upper limit permitted for most industrial facilities (25% of the lower explosive limit (LEL)).

5. NREL had previously estimated the COO for photocatalytic oxidation based on its current photocatalyst to be approximately \$35,000 per thousand CFM treated (Notarfonzo and McPhee 1994). The smaller value they report in the Sematech study results from the change in the design basis from acetone to methanol; methanol is easier to treat via PCO, so the resulting system is less expensive to purchase and to operate.
6. The Sematech study suggests that the conclusions drawn regarding the relative costs of PCO and catalytic oxidation systems be used with caution. The thermal catalytic oxidation cost estimates are actual system quotes for readily available, existing systems. Moreover, thermal catalytic oxidation is a well-understood, widely used, robust technology that has been successfully applied to many systems. In contrast, PCO systems are a new technology, with scant data available on the long-term reliability and operational concerns.
7. PCO technology, like other catalytic technologies, is not suited for VOC emissions containing hexmethyldisilazane (HMDS) because of rapid catalyst deactivation, which would lower the overall performance of the POU technology.

Sizing Approach & Cost Analysis - Based on EPA Authored Report

Henschel (1998) published a cost comparison for an indoor air cleaner operating at a flow rate of $1 \text{ m}^3 \text{ sec}^{-1}$ ($= 2120 \text{ ft}^3 \text{ min}^{-1}$) using granular activated carbon (GAC) versus photocatalytic oxidation (PCO) for treating a steady-state inlet VOC concentration of 0.27 mg m^{-3} . The price of the commercial GAC unit was estimated by assuming the inlet VOCs had reasonable carbon sorption affinities that were representative of compounds having four or more atoms (exclusive of hydrogen). A model for the PCO unit was designed and cost-estimates were developed using VOC oxidation rate data reported in the literature for the low inlet concentrations and using typical illumination intensity. Key assumptions used in the analysis for both the GAC and PCO units are shown in Table 5.

Because of limited information available regarding the proprietary designs of firms marketing PCO systems, the cost analysis for the PCO unit in this study (Henschel 1998) is a model and not to be considered rigorous. Based on a review of the published literature of PCO reactor designs, the PCO unit

in this study employed a V-shape, with UV bulbs positioned in the front and rear of the panel beds to illuminate the catalyst. It is noted that the model PCO design developed here is different than those being offered commercially. That is, it includes drawbacks, e.g., the V-bank panel configuration will diminish the distribution of UV radiation into the interior of the substrate matrix.

Installed Cost. The study reveals that the installed cost of the model PCO reactor is \$16,310, resulting from the high cost of the PCO reactor and catalyst, and from the significant increase in HVAC cooling capacity required to remove the heat added by the UV bulbs and ballasts (Table 6). The study (Henschel 1998) mentions that the source of the largest uncertainty in the cost is the fabrication and installation costs.

Annual Cost. The study (Henschel 1998) demonstrates that the total annual cost associated with the POR is \$11,800 (Table 7). The two largest contributions to the annual PCO cost result from the UV bulbs – electricity to operate the bulbs and bulb replacement. The study suggests that the \$2,370 annual cost of bulb replacement in the POR could conceptually be reduced if it was possible to use low-pressure fluorescent bulbs having a reported 10,000 h lifetime as a substitute for the 1,000-h-medium-pressure bulbs.

Study Summary. The investigation (Henschel 1998) states that due to the large amounts of ultraviolet (UV) energy and catalyst surface areas required, PCO units are likely to be very expensive for removing VOCs from indoor air. Unless improved catalysts can be developed that substantially reduce energy and surface requirements, PCO is not likely to increase the utilization of air cleaners for indoor VOC control, or to challenge GAC as the most common VOC air cleaning method. Cost will likely limit PCO to specialized indoor applications where GAC is not an option (e.g., because the specific compound is poorly sorbed on carbon). Additional concluding statements include: (1) the PCO installed cost decreases approximately linearly with decreases in the required catalyst surface area and UV power. The area and power decrease inversely with the reaction rate. Thus, even with extremely optimistic assumptions regarding system design innovation and reduced component costs, the PCO reaction rate at 1 ppmv would

still have to be increased almost threefold, to about $0.3 \mu\text{mol h}^{-1} \text{cm}^{-2}$ at 1mW cm^{-2} , to match the GAC cost estimate. With the base-line costs of the model PCO reactor, the rate would have to be increased by more than 10-fold, to over $1 \mu\text{mol h}^{-1} \text{cm}^{-2}$ at 1mW cm^{-2} ; and (2) improved catalysts will be necessary to achieve these faster rates. To provide faster rates, with the corresponding reduction in power requirements, the improved catalyst will have to offer higher quantum efficiencies, above the value ($\sim 0.1\%$) at the conditions assumed here. A greater percentage of the UV photons must become effective in oxidizing VOC molecules, or PCO will remain an energy-intensive and expensive process.

CONCLUSION

The results of several approaches to estimate the cost of installing and operating a PCO device for application in various treatment concerns are presented. First, a simplified approach for estimating the cost of a PCO treatment device using laboratory data is presented in some detail. The approach is limited to conditions where the intent is to remove a gas-phase contaminant in a space from an initial concentration to a final concentration over a given treatment period and in the absence of contaminant generation within the space. Second, the cost of ownership of a PCO device operating at 700 scfm for treating outgases from soils contaminated with liquid solvents is compared with other treatment technologies – soil vapor extraction with granular activated carbon, and groundwater extraction with liquid phase UV/peroxidation. The PCO device is shown to have a significant 30-year net present cost savings over the other treatment technologies. Third, a study based on a consortium of semi-conductor companies demonstrated that the cost of ownership of a PCO for POU applications is not likely to cost less on a “per CFM basis” than existing EOP technologies. However, the study findings indicated that in a number of specific cases PCO may provide a cost-effective alternative to EOP technologies. Last, a report was published comparing the first and operating costs of PCO vs. GAC at a flow rate of $1 \text{m}^3 \text{sec}^{-1}$ ($= 2120 \text{ft}^3 \text{min}^{-1}$). The study reported that due to the high first and operating costs of PCO device compared with the GAC approach, PCO is not likely to replace GAC as a technology for treating a steady-state inlet

feed of VOCs. The study concluded that PCO can improve in this comparison (to GAC) if improved catalysts capable of high reaction rates and quantum yields are developed.

ACKNOWLEDGEMENTS

The authors of this report would like to thank Prof. Michael Zorn of the Environmental Chemistry and Technology Program at the University of Wisconsin-Green Bay for discussions pertaining to PCO reactor modeling. Gratitude is extended to the numerous businesses with which I spoke regarding their present and future capabilities in marketing commercial-scale photocatalytic treatment technologies. This project was supported through ASHRAE research project 1134-RP.

NOMENCLATURE

<u>Variable</u>	<u>Description</u>	<u>Units</u>
C	concentration of (gas) species in the zone	mol L^{-1}
C_A	concentration of (gas) species A in the zone	mol L^{-1}
C_{A0}	initial concentration of (gas) species A	mol L^{-1}
k_A	reaction rate constant of species A	dependent on n
n	reaction order – based on power law model	dimensionless
r_A	rate of disappearance of species A	$\text{mol s}^{-1} \text{ g}^{-1}$
<i>slope</i>	slope of regression plot	dependent on plot
t	time	s
V_{res}	Volume of reservoir	L
W	mass of photocatalyst	g

REFERENCES

- Brunet, R.A.H., R. Pearcey, J.R. Kittrell, G. Mackin, and C.A. Wise. 1999. Site remediation using photocatalytic VOC destruction of chlorinated hydrocarbons. *Proceedings of the Air & Waste Management Association's Annual Meeting*, June 20-24, 1999, St.Louis, MO. vol. 99-826.
- Edwards, M.E. 1994. Kinetics and intraparticle mass transfer limitations in photocatalytic systems. PhD thesis. University of Wisconsin. Madison, WI.
- Henschel, D.B. 1998. Cost analysis of activated carbon versus photocatalytic oxidation for removing organic compounds from indoor air. *J. Air & Waste Manage. Assoc.* 48(10):985-994.
- Moretti, E.C. and N. Mukhopadhyay. 1993. VOC control: Current practices and future trends. *Chem. Engr. Progress* July 1993:20-26.
- Notarfonzo, R. and W. McPhee. 1994. How to evaluate a UV/oxidation system. *Pollution Engr.* October:74-76.
- Turchi, C.S., E.J. Wolfrum, and R.A. Miller. 1994. Gas-phase photocatalytic oxidation: Cost comparison with other air pollution control technologies. Golden, CO. NREL. NREL/TP-471-7014.
- Turchi, C.S., R. Rabago, and A. Jassal. 1995. Destruction of volatile organic compound (VOC) emissions by photocatalytic oxidation (PCO): Benchscale test results and cost analysis. Sematec, Inc. Technology Transfer 95082935A-ENG.
- Wolfrum, E.J., R. Rabago, and A.S. Jassal. 1997. Destruction of volatile organic compound (VOC) emissions by photocatalytic oxidation (PCO): Final Report (ESHCOO3). Austin, TX. Sematch, Inc. 97013236A-ENG.
- Zorn, M.E., D.T. Tompkins, W.A. Zeltner, and M.A. Anderson. 2000. Catalytic and photocatalytic oxidation of ethylene on titania-based thin-films. *Environ. Sci. Technol.* 34:5206-5210.

TABLE HEADINGS

Table 1 Data from PCO experiment.

Table 2 Cost of USEPA Remedy (adapted from Brunet et al. 1999)

Table 3 Cost of UV Alternative – Corporate Entity (adapted from Brunet et al. 1999)

Table 4 Results of Sematech COO Analysis for 1000 CFM, 500 ppmv methanol POU treatment
System Option (adapted from Wolfrum et al. 1997)

Table 6 Installed costs of a PCO VOC air cleaner. (Reproduced, in part, from Table 5 in Henschel 1998.)

Table 7 Annual costs of a PCO VOC air cleaner. (Reproduced, in part, from Table 6 in Henschel 1998.)

TABLES

Table 1

Clock Time (hr:min)	Elapsed Time (min)	Ethylene (Gas) Concentration (ppmv)
12:20	0	9.5
13:20	60	7.85
14:18	118	6.5
15:40	200	4.7
17:25	305	3.15
20:30	490	1.4
23:10	650	0.7
6:30	1090	0.07

Table 2

<u>Soil Vapor Extraction with Vapor Phase Granular Activated Carbon (GAC)</u>		<u>Source</u>
Capital Cost		
Complete System: Wells, Extraction and Treatment	\$480,000	Remedial Design Estimate
Operating/Maintenance Costs		
Duration	4 yr	
GAC (including disposal)	\$87,500/yr	Remedial Design Estimate
Soil monitoring	\$31,750/yr	Vendor quotation
O&M labor/analytical	\$144,000/yr	Vendor quotation
Total Cash Flow	\$263,250/yr	Remedial Design Estimate
NPC of O&M	\$891,680	
Total Net Present Cost	\$1,371,680	
Groundwater Extraction with Liquid Phase UV/Peroxidation		
Capital Costs		
Complete System: Extraction and Treatment	\$868,200	Remedial Design Estimate
Operating/Maintenance Costs		
Duration	30 yr	
Hydrogen Peroxide	\$50,400/yr	Remedial Design Estimate
UV Lamps	\$15,600/yr	Vendor quotation
Electricity	\$90,200/yr	Vendor quotation
Groundwater Monitoring	\$25,200/yr	Remedial Design Estimate
Total Cash Flow	\$181,200/yr	
NPC of O&M (7%, 30 yr)	\$2,248,511	
	\$891,680	
Total Net Present Cost	\$3,116,711	
Total Net Present Cost USEPA Remedy	<u>\$4,488,391</u>	

Table 3

<u>Soil Vapor Extraction with Gas Phase UV Photocatalysis</u>		<u>Source</u>
Capital Cost		
Complete System: Wells, Extraction and Treatment	\$480,000	Actual expenditures, including saturated zone liquid/vapor extraction, and one-time design/development costs
Operating/Maintenance Costs		
Duration	4 yr	Actual expenditure, 1998
GAC (including disposal)	\$6,000/yr	Vendor quotation
Photocatalytic Electricity	\$6,000/yr	Actual expenditure, 1998
Caustic (neutralizes HCl)	\$1,500/yr	Vendor quotation, operations
Catalyst/lamp replacement	\$14,800/yr	EPA Record of Decision
Soil Monitoring	\$31,750/yr	Vendor quotation
O&M labor/analytical	\$75,000/yr	
Total Cash Flow	\$135,0500/yr	
NPC of O&M (7%, 4 yr)	\$457,441	
Total Net Present Cost	\$1,345,641	Neglects extraction pump head costs.
<u>Soil Vapor Extraction with Air Stripping and Gas Phase UV Photocatalysis</u>		
Capital Cost		
Extraction pumps, field piping, treatment building	\$480,000	Actual expenditures
Operating/Maintenance Costs		
Duration	30 yr	
Electricity	\$17,000/yr	Remedial Design Estimate
Caustic (neutralizes HCl)	\$1,000/yr	Projected based on 1998
Catalyst/lamp replacement	\$14,133/yr	Vendor quotation
Groundwater Monitoring	\$25,000/yr	Remedial Design Estimate
O&M labor/analytical	\$30,000/yr	Projected based on 1998
Total Cash Flow	\$57,133/yr	
NPC of O&M (7%, 4 yr)	\$708,968	
Total Net Present Cost	\$958,968	
Total Net Present Cost Corporate Entity	<u>\$2,304,609</u>	
<i>Total Net Present Cost Difference</i>	<u>\$2,183,782</u>	

Table 4

Quote Source		Capital Cost (\$K)	Electric Load (kW)	Fuel Load (MMBTU/hr)	COO (\$/scfm)
NREL	PCO	60	5.0	0.1	228
Corporate entity #1 ⁽¹⁾	PCO	46	6.9	0	23
Corporate entity #2	Thermal	127	9.4	1.0	58
	Catalytic				
Corporate entity #3	Thermal	80	1.2	0.22	34
	Catalytic				

⁽¹⁾Quote is for a 50 ppmv methanol treatment system.

Table 5

Parameter	Assumed Value
Building outdoor air ventilation rate (mechanical plus infiltration)	10 L/s of outdoor air/person
VOC concentration in outdoor air	0
Indoor air recirculation rate through air handler (and air cleaner)	7 air changes/hr
VOC generation rate inside building	5 mg VOC/hr/m ² floor air (resulting in indoor air concentration of 0.5-1.1 ppmv in the absence of an air cleaner.)
Required VOC removal efficiency	Reduce indoor air concentration by 85% to 0.3 mg/m ³
Nature of building	New construction; no retrofit costs
Year of installation	1996
Escalation (inflation) rate	5%
Interest rate	8%
Equipment lifetime and depreciation	10-year lifetime; straight-line depreciation
Insurance and real estate taxes	2% of original investment
Cost of electricity	\$0.0473/kWh plus a demand charge of \$9.96/kWh for usage rates greater than 10 kW
Air cleaner operating hours	273 hr/month (off overnight, weekends)
HVAC system characteristics	Packaged VAV system; fan static pressure of 870 Pa, in absence of air cleaner.

Table 6

Cost Item	Installed Cost (\$/m³/s capacity)
Reactor (excluding catalyst)	\$ 8,090
Initial amount of catalyst	6,480
Enlarged central air handler (to handle increased static pressure)	20
Increased cooling capacity (to cool air stream that is heated inside an enlarged air handler)	1,720
Total	\$ 16,310

Table 7

Cost Item	Annual Cost (\$/yr/m³/s capacity)
Operating Costs	
Electricity (for increased fan static pressure, cooling load, UV bulbs)	\$ 4,440
Maintenance	
Regeneration of catalyst	\$ 1,510
Replacement of UV bulbs	2,370
Replacement of PCO final filter	20
Indirect Expenses	
Depreciation of equipment (10 yr)	\$ 980
Depreciation of catalyst (5 yr x 2)	\$ 1,500
Insurance and real estate taxes	330
Interest on capital (installed cost)	650
Total	\$ 11,800

FIGURE CAPTION SHEET

- Figure 1 Methodology for developing commercial-scale prototype photocatalytic reactor from laboratory data.
- Figure 2 Approximation of conversion data with $n = 1/2$ (power law) kinetic model. Data are points and line is approximation with kinetic model.
- Figure 3 Approximation of conversion data with $n = 4/5$ (power law) kinetic model. Data are points and line is approximation with kinetic model.
- Figure 4 Mass of photocatalyst required in photo-reactor versus volume of enclosure (e.g, building). $C_A = 0.05 C_{A0}$; $k_A = 6.99 \times 10^{-3} \text{ mol}^{1/5} \text{ L}^{4/5} \text{ g}^{-1} \text{ s}^{-1}$; $t = 86,400 \text{ s}$ (1 day) with $n = 4/5$.
- Figure 5 Mass of photocatalyst required in photo-reactor versus volume of enclosure (e.g, building). $C_A = 0.05 C_{A0}$; $k_A = 6.99 \times 10^{-1} \text{ mol}^{1/5} \text{ L}^{4/5} \text{ g}^{-1} \text{ s}^{-1}$; $t = 86,400 \text{ s}$ (1 day) with $n = 4/5$.
- Figure 6 Capital cost of POR for a given treatment volume (V_{res}). $C_A = 0.05 C_{A0}$; $k_A = 6.99 \times 10^{-3} \text{ mol}^{1/5} \text{ L}^{4/5} \text{ g}^{-1} \text{ s}^{-1}$, $t = 86,400 \text{ s}$ (1 day) with $n = 4/5$.
- Figure 7 Capital cost of POR for a given treatment volume (V_{res}); for oxidizing a gas with a rate constant 2 orders of magnitude less than that for ethylene. $C_A = 0.05 C_{A0}$; $k_A = 6.99 \times 10^{-1} \text{ mol}^{1/5} \text{ L}^{4/5} \text{ g}^{-1} \text{ s}^{-1}$, $t = 86,400 \text{ s}$ (1 day) with $n = 4/5$.

FIGURES

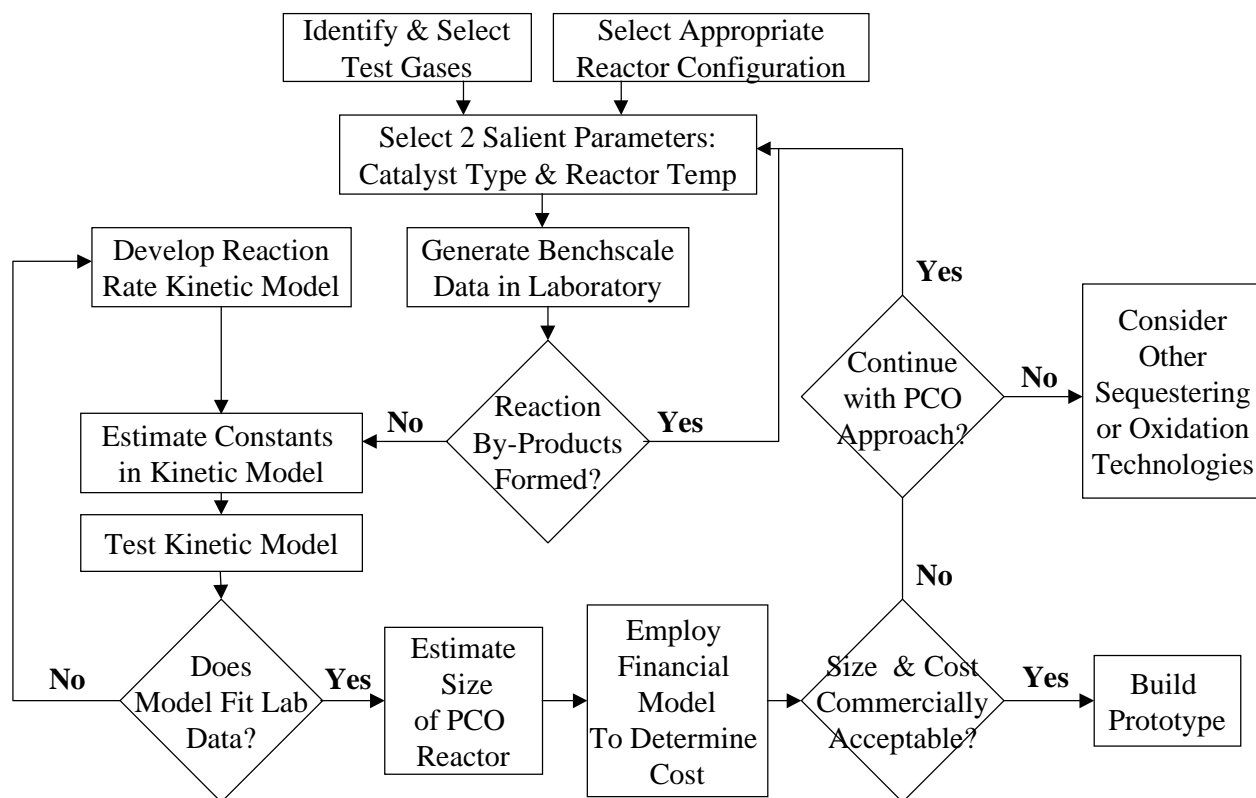


Figure 1

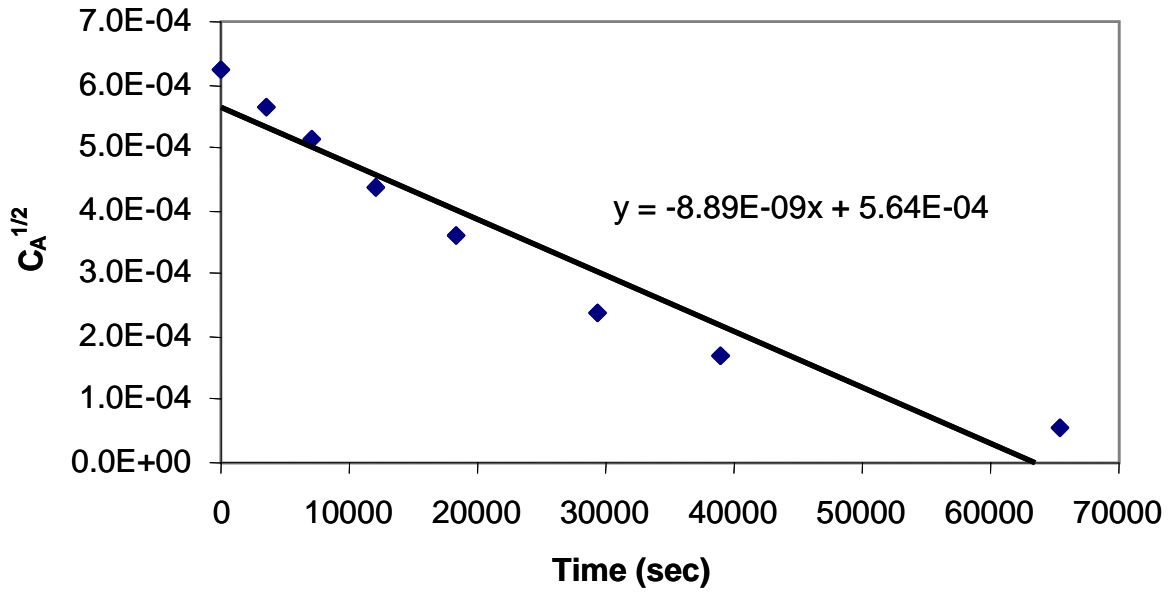


Figure 2

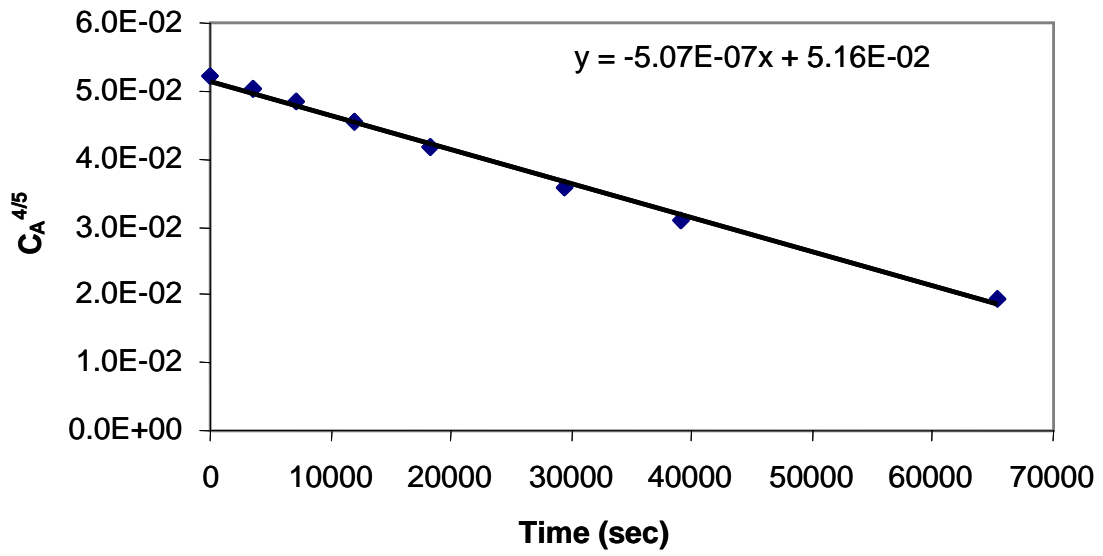


Figure 3

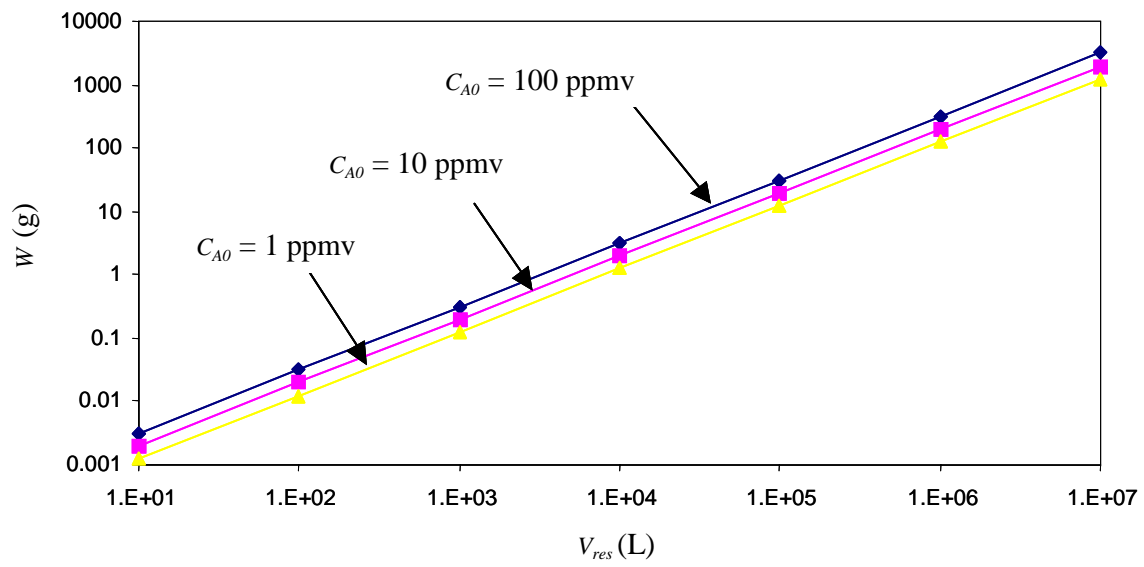


Figure 4

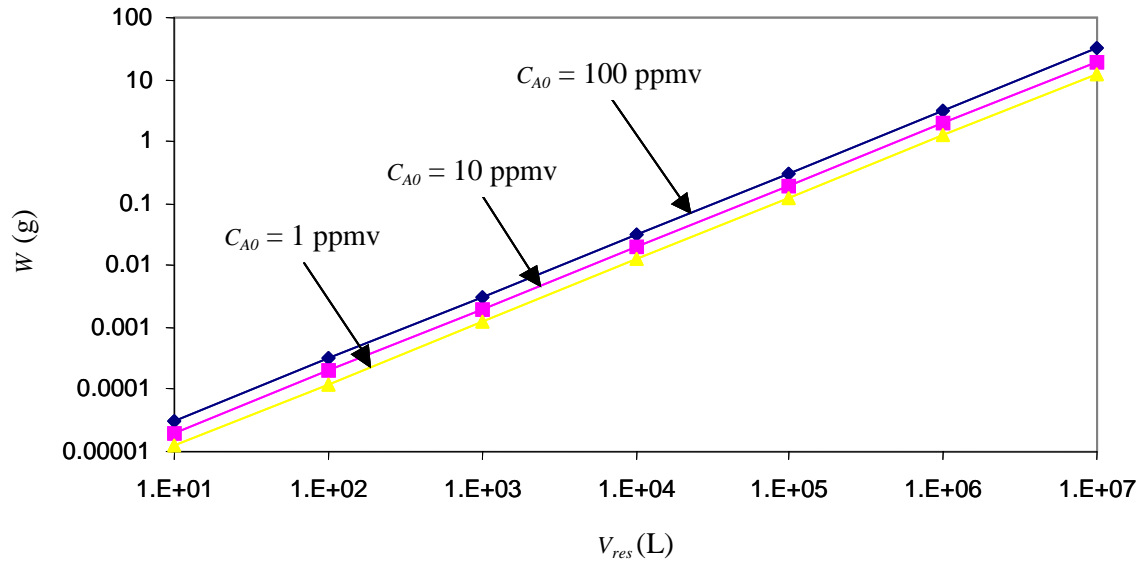


Figure 5

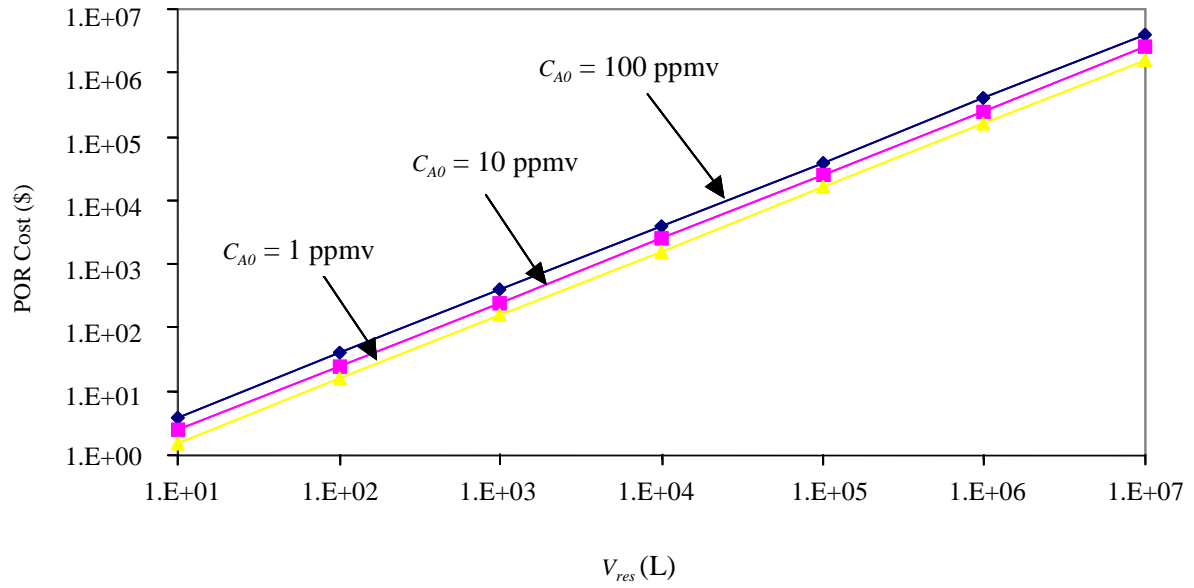


Figure 6

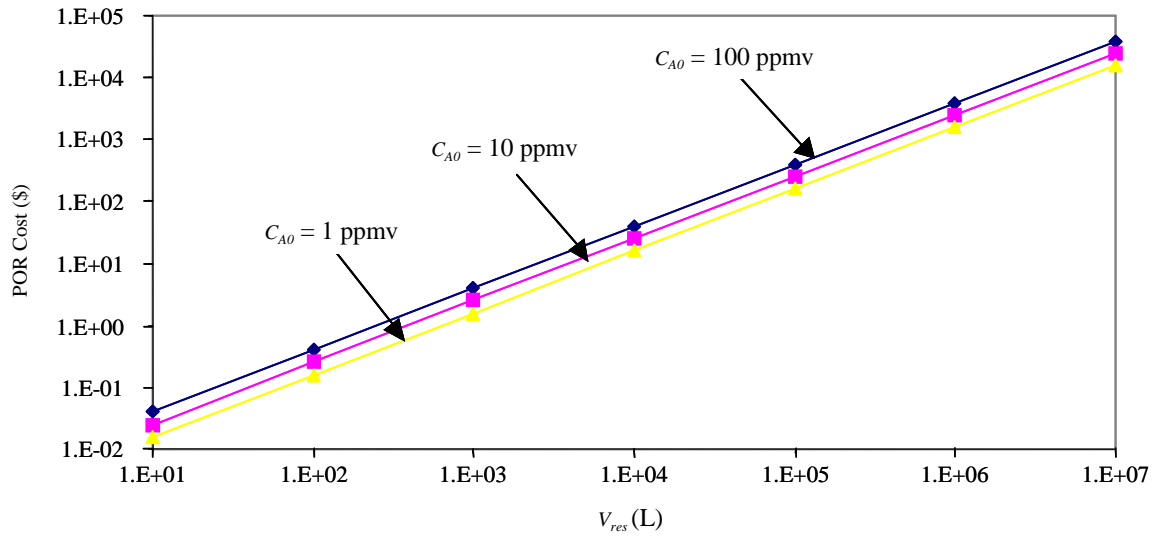


Figure 7